Max-Planck-Institut für Meteorologie

REPORT No. 243

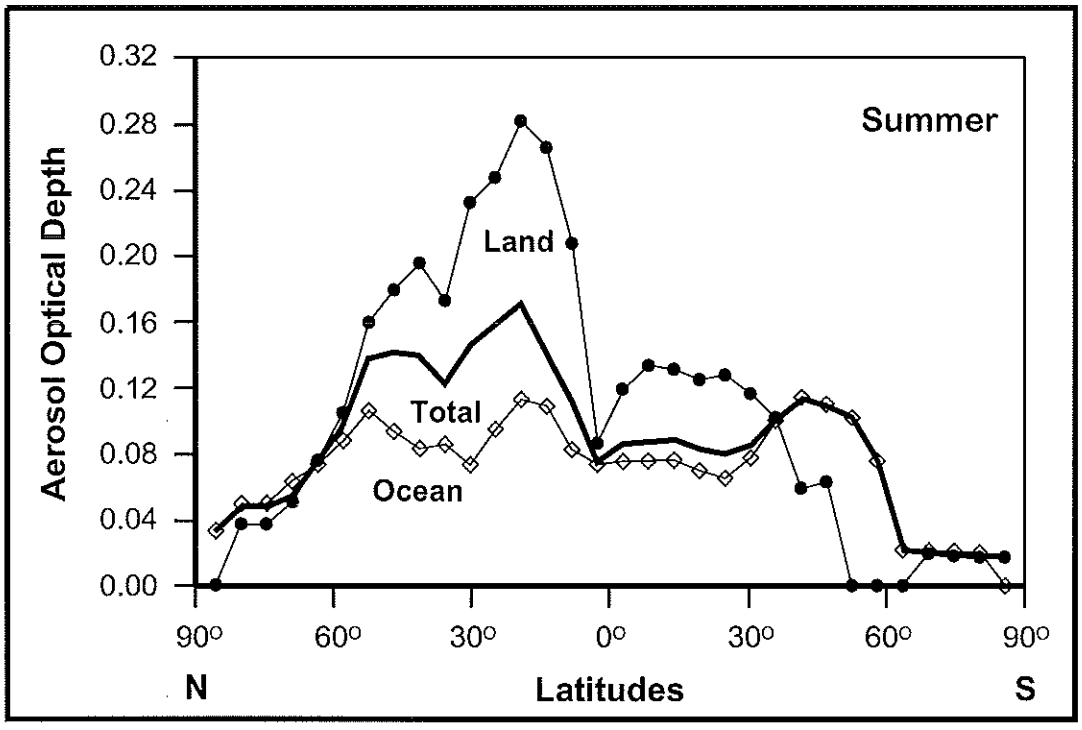

GLOBAL AEROSOL DATA SET

by

Peter Köpke • Michael Hess
Ingrid Schult • Eric P. Shettle

HAMBURG, September 1997

AUTHORS:

Peter Köpke
Michael Hess

Meteorologisches Institut
der Universität München
Theresienstr. 37
D-80333 München
Germany

Ingrid Schult

Max-Planck-Institut
für Meteorologie
Bundesstr. 55
D-20146 Hamburg
Germany

Eric P. Shettle

Code 7227
Remote Sensing Division
Naval Research Laboratory Washington
D.C. 20375-5351
USA

MAX-PLANCK-INSTITUT
FÜR METEOROLOGIE
BUNDESSTRASSE 55
D - 20146 HAMBURG
GERMANY

Tel.: +49-(0)40-4 11 73-0
Telefax: +49-(0)40-4 11 73-298
E-Mail: <name> @ dkrz.de

REPb 243

GLOBAL AEROSOL DATA SET

P. Koepke, M. Hess,

Meteorologisches Institut der Universitaet Muenchen
Theresienstrasse 37, D-80333 Muenchen, Germany

I. Schult, and

Max-Planck-Institut für Meteorologie
Bundesstrasse 55, D-20146 Hamburg, Germany

E. P. Shettle

Code 7227, Remote Sensing Division
Naval Research Laboratory Washington, D.C. 20375-5351

ISSN 0937-1060

0 Abstract

For climate change investigations it is necessary to include the influence of aerosol particles with their temporally and spatially variable properties in addition to the known effects of greenhouse gases. Global fields of all optical parameters necessary for an estimate of the radiative forcing by aerosol particles and to quantify the resulting climate effects are not available from measurements due to the multiple influence parameters. Therefore, aerosol data globally existing from different measurements and more extensive models have been compiled into the Global Aerosol Data Set (GADS).

In the GADS presented here, the atmospheric aerosol particles are described by 10 main aerosol components which are representative for the atmosphere and characterised through their size distribution and their refractive index depending on the wavelength. These aerosol particles are based on components resulting from aerosol emission, formation and removal processes within the atmosphere, so that they exist as mixture of different substances, both external and internal. Typical components include water-soluble, water-insoluble, soot, sea-salt and mineral. The sea salt particles are defined in two size classes and the mineral particles in four.

For these chosen components the radiative properties are calculated by means of Mie theory at wavelength between 0.3 and 40 µm and for 8 values of relative humidity. In addition to the optical properties, the global aerosol distribution of each defined aerosol component including the vertical profile has been determined by the GADS on a 5°×5° latitude-longitude grid for winter and summer. This permits the determination of the radiative properties and mass concentration of the resulting externally mixed aerosols at each grid point on the globe.

1 Introduction

Atmospheric aerosols are a significant source of direct climate forcing (e.g. Grassl, 1988; Penner et al., 1994; Lacis and Mischenko, 1995) and perhaps the greatest uncertainty in climate forcing is that due to tropospheric aerosols (Hansen, 1993). Scattering of tropospheric anthropogenic aerosols causes a clear-sky forcing, which on the average is comparable in magnitude but opposite in sign to forcing by anthropogenic greenhouse gases (Hansen and Lacis, 1990; Charlson et al., 1992) and thus are responsible for at least partially masking the warming due to past greenhouse gas increases.

However, unlike greenhouse gases, aerosol particles exhibit significant temporal and spatial variations, both in amount and properties, and, moreover, the direct aerosol radiative forcing depends on solar elevation and surface albedo. Thus, it is desirable to include the aerosol effects in global circulation models with the aerosol properties changing with time and position in the atmosphere. Detailed process oriented aerosol microphysical models to track the evolution of the aerosol properties and concentration, in addition to and depending on the meteorological parameters, are available only for a few aerosol types. Thus the use of average aerosol properties even now is a good method for the investigation of direct climatic effects of tropospheric aerosol particles, both natural and anthropogenic. A way to describe aerosol properties which considers both their different sources and their modifications during stay in the atmosphere is external mixing of internally mixed components (WMO, 1983).

This approach is utilized to describe aerosol properties in the Global Aerosol Data Set (GADS) with the mixing ratios depending on season and place. Data are given for summer and winter on a global grid with 5° longitude and latitude spacing. GADS is a completely revised version of the aerosol climatology developed by d'Almeida et al. (1991). Data of GADS are internally consistent with respect to aerosol mass per volume and optical properties and they appear to be comparable with different regional in situ and ground based measurements and satellite data, as well directly aerosol as radiation observations. The properties of the aerosol components are available and easy to handle in the software package Optical Properties of Aerosols and Clouds (OPAC) (Hess et al., 1996). OPAC gives the possibility to model climate relevant optical properties of any mixture of clouds and aerosols for individual cases.

It must be emphasised, that aerosol observations made on different places on earth are not at all adequate for a precise description of their global spatial and temporal radiative properties

(e.g. Heintzenberg, 1989; Bashurova et al. 1992; Pinnick et al. 1993; Hänel, 1994). Moreover, measured data sets are seldom complete with respect to all quantities and wavelengths which are necessary for climate modelling. Thus, a possible way is to combine different information both of optical and of microphysical measurements, with the use of different components and their mixture. This is consistent with the current limitations on our knowledge of the atmospheric aerosols. Measuring campaigns are too infrequent, in comparison with the high variability of tropospheric aerosol due to its short life time, with the consequence that the conditions at a specific location and time can differ from the results in GADS by more than an order of magnitude. But the data are a useful tool for aerosol sensitivity studies and for use in GCMs.

2 Modelling needs and realisation

The direct climatic impact of aerosols is due to their modification of atmospheric radiation balance at all wavelengths with a reduction of the solar irradiance reaching the lower atmosphere and surface as a consequence of aerosol backscatter and with atmospheric heating as consequence of aerosol absorption. To calculate these effects with a suitable radiative transfer model as function of location on earth (x,y), height in the atmosphere (z), time (t), it is necessary to have the wavelength (λ) dependent aerosol radiative parameters: extinction coefficient σ_e, single scattering albedo ω_0 and phase function $P(\theta)$ or at least the asymmetry factor g.

At present, such data over the full range of solar and thermal wavelengths neither are available from in-situ measurements, nor from remote sensing. The only way is to compute them with light scattering theory (usually Mie theory) from the aerosol size distribution and the wavelength dependent refractive index. To allow for the problem of internal and external mixing of particles of different origin (WMO, 1983), an adequate way to describe the total aerosol is adding of internally mixed aerosol components with time and site dependent amounts of the number of particles of each of the components. This procedure is extremely flexible and allows, if improved information is available, to change the properties of individual components e.g. size distribution, refractive index or effect of relative humidity without changing the others. Also the mixing ratio or the total amount of particles easily can be improved or further components can be added if necessary. Combining the individual components in this manner allows the climate model to follow or model the evolution of

aerosol components separately or to model selected aerosol components (e.g. soot), and utilize the default GADS global climatology for the others. Also use of scattering theories which consider properties of nonspherical particles is possible, but not yet done. This may be part of future improvements as well the variation of properties or amount of components as function of meteorological parameters, calculated by the climate model.

In the present version of GADS, ten aerosols components are used to describe the aerosol. In general, these are the components already used in d'Almeida et al. (1991) and WMO (1983) with some improvements mentioned below. From these components the aerosol is mixed to averages valid for a grid of 5° longitude and latitude and both for summer (June, July, August) and winter (December, January, February).

To get information on the relative amount of the components, information from optical measurements like spectral extinction coefficients (Ångström parameters) and single scattering albedo and from microphysical measurements like radius dependent mass or chemical composition is used. Optical measurements like visibility, extinction coefficient, optical depth and microphysical measurements like total particle mass are used to derive the total aerosol amount.

In-situ measurements in any case are available only from few locations, often in the vicinity of cities, and for short time periods and specific weather conditions. Thus the averages in space and time only are estimated. To fill the grid on the global scale moreover similarity considerations are used and descriptive information, like the vegetation type and the days with blowing dust.

3 General description

The tropospheric aerosols are described by an external mixture of internally mixed aerosol components. In the GADS, 10 aerosol components are defined characterised through the particle size distribution and the wavelength dependent index of refraction. The aerosol particles are based on components which result from aerosol emission, formation and removal processes within the atmosphere, so that they exist as mixture of different substances, both external and internal. The choice of 10 components is a compromise between the need for detailed information and the possibility to get it. The components and the parameters to describe their microphysical properties of are given in Table 1. Detailed information on the components is given in the next chapter.

The size distribution of each component is given as log-normal distribution with r_m the mode radius, σ the geometric standard deviation to describe the width of the distribution and N the particle number density of the component (in particles/cm^3).

$$\frac{dN(r)}{d\log r} = \frac{N}{\sqrt{2\pi}\cdot\log\sigma}\exp\left(-\frac{1}{2}\left(\frac{\log r - \log r_m}{\log\sigma}\right)^2\right) \tag{3.1}$$

The volume V of one particle, which represents an average of the component is given with Equation (3.2) if integrated over all radii.

$$V = \frac{4}{3}\ \pi\ r_m^3 \exp\ [\frac{9}{2}\ \ln\sigma] \tag{3.2}$$

The mass M of one average particle is given by its volume multiplied with its specific density ρ

$$M = V\cdot\rho\ . \tag{3.3}$$

For each of the components, the complex refractive index is given as bulk property. That means, a homogeneous internal mixture of the different chemical substances which form the particles is assumed. For materials in solution with water this is a valid assumption. The spectral dependence of the refractive indices of dry particles is illustrated for the different components in Figure 1, the real and imaginary part, respectively. It is obviously that, except for soot, both parts of refractive index show a strong spectral variance, especially at near and far infrared wavelengths.

Hygroscopic and deliquescent particles grow with increasing relative humidity. With the relative humidity aerosol particles change their size, their density and their refractive index as the dry particulate matter can be assumed to be mixed with water. Since the crystallisation humidity for most salts and salt mixtures which form natural hygroscopic aerosols is less then 40 % relative humidity (Winkler, 1973; Shaw and Rood, 1990), under natural conditions the hysteresis in the particle humidity growth curve due to different deliquescence and crystallisation humidity usually can be ignored. Thus a model after Hänel and Zankl (1979) for equilibrium conditions is used to describe the correlation between aerosol size and relative humidity. The humidity dependent size of the particles of each component is taken into account by the changing mode radii as function of relative humidity, but leaving the standard deviation σ unchanged. Table 2 gives mode radii r_m and specific densities ρ for the hygroscopic components for 8 humidity classes. Note that the particle radius already is

increased at 50 % relative humidity, because 0 % is a theoretical value, and not equal to dry from laboratory conditions, which is about 30 % or more.

Density and refractive index m* (both real and imaginary part) of the particles under humid conditions are calculated, under the usual assumption that the volume of the water and the dry particle are additive in the solution droplets, by

$$\rho = \rho_{dry} \frac{r_{m_{dry}}^{3}}{r_m^{3}} + \rho_{water} \frac{r_m^{3} - r_{m_{dry}}^{3}}{r_m^{3}}$$

$$m^* = m^*_{water} + (m^*_{dry} - m^*_{water}) \frac{r_{m_{dry}}^{3}}{r_m^{3}} \qquad (3.4)$$

with $r_{m\,dry}$ is the mode radius of the dry particle and r_m the mode radius at the definite relative humidity.

The particle volume and mass presented in Table 3 for 8 values of relative humidity, is given both under the assumption of a cut off radius of 7.5 μm and with the assumption of no radius limitation in Equation 3.2. The effect of such a cut off is shown, because most measurements have some kind of cut off, which can make a significant difference between the measured and the actual mass concentration. This is essential in cases with high amount of large particles, as over deserts and over ocean. For the calculation of radiative properties, of course, no cut off is taken into account.

The radiative properties of each of the components are calculated with Mie-theory (computer program by Quenzel and Müller, 1978) under the assumption that the particles are spherical for 60 wavelengths in the range between 0.25 μm and 40 μm. To calculate the optical properties, mostly a lower limiting radius of 0.005 μm and an upper limiting radius of 20 μm is used. Coarse mode particles, sea-salt coarse mode and mineral coarse mode, are modelled with upper radii of 60 μm in the dry case because such large particles really are collected (d'Almeida 1987; Coude-Gaussen et al., 1987; Dekker and de Leeuw, 1993). The lower and upper bounded radii for Mie-calculation also are changed with relative humidity.

Usually tropospheric aerosol consists of particles of different origin. Thus, as mentioned, for this data base the aerosol at a given location is composed by combing from one to four components (denoted by an index i) each with different particle number concentration N_i , [particle per cubic-centimeter, cm^{-3}]. One particle of a component in this sense is an averaged particle, which describes the optical properties of the total component, integrated over radii. This is the most direct way to model aerosol mixtures and in addition allows easily to take into accounts effects of relative humidity, which are different for the different components in a

mixture. The aerosol mixtures should be individual for each place, given by the individual number of particles of each of the components. This is better than a description by a fixed mixing ratio of the components in combination with the total number of particles, because usually with a change of the total amount of particles, i.e. the turbidity, also the relative contribution of the different components changes.

The size distribution of the total aerosol in every case is added from its components using the individual particle numbers N_i .

$$\frac{dN(r)}{d(\log r)} = \sum_i \frac{dN_i(r)}{d(\log r)} \qquad (3.5)$$

This adding is also correct for total particle number and mass concentration.

Since aerosol particles interact independently with the radiation field, the extinction-, scattering- and absorption coefficients for total aerosol are obtained by summing up the coefficients of the components, under consideration of the individual particle number. The single scattering albedo, T_0 , and the asymmetry factor, g, valid for the total aerosol, are obtained as weighted averages of the corresponding values for the individual components. They must be weighted by extinction coefficient respectively scattering coefficient

$$\omega_0(\lambda) = \sum_i \omega_{0_i}(\lambda) \cdot \sigma_{e_i}(\lambda) / \sum_i \sigma_{e_i}(\lambda) \qquad (3.6)$$

$$g(\lambda) = \sum_i g_i(\lambda) \cdot \sigma_{s_i}(\lambda) / \sum_i \sigma_{s_i}(\lambda) \qquad (3.7)$$

Since the mixture of components is highly variable, radiative properties for total aerosol are given later as global maps.

4 Microphysical and optical data of aerosol components

The properties of the 10 aerosol components used in the GADS are discussed in the following section. The components are water-insoluble, water-soluble, soot, sulfate droplets, sea-salt and mineral, in which the last two exist in different size classes. The size parameters are given in Table 1, the refractive index for dry particles in Figure 1 and humidity dependent properties in Table 2 as introduced before. Representative optical parameters - mass extinction efficiency, single scattering albedo, and the asymmetry factor of the scattering function - calculated by Mie programme are plotted in Figure 2 for the relative humidity of 50% as function of

wavelength. Additionally, for selected wavelengths of 0.5 μm and 10 μm, in the Table 4 the optical parameters are given.

The mass extinction efficiencies are calculated under the assumption, that the extinction coefficient is valid for the airborne particles, that is with the limiting radii mentioned above, but the mass is determined by a probe and the cut off radius is taken into account. Thus, the values are much larger than if the mass used is calculated from size distributions with no radius limit. Given the strong dependence of mass optical efficiencies on the density and volume, it is indeed important to take note of which parameters are measured or modelled and how.

The optical parameters in Figure 2 show a strong spectral dependence on the aerosol component which results from both spectral refractive index and the size distribution. The extinction (Figure 2a) exhibits a strong decrease with increasing wavelength, for the smaller sized WASO, SOOT and SUSO particles, in the visible spectral range but nearly constant values for bigger particles such as SSAM, MIAM and INSO. Basically, the single scattering albedo shown in Figure 2b, depends on the imaginary part of the refractive index. If this value is low, the particle is only a weak absorber and the single scattering albedo is close to one as for sea-salt (SSAM), SUSO and WASO at the short wave spectrum. At large wavelengths all components are absorbing, as the SOOT, the INSO and the mineral aerosols are more or less already in the visible, with the consequence of low single scattering albedo. The low values at 3 μm for the hygroscopic components result from water absorption at this wavelength, which takes place since the values in Figure 2 are calculated for 50 % relative humidity.

The asymmetry factor is a measure of the forward scattering properties of the particles, and it's behaviour is dominated by the particle size relative to the wavelength. It is high for large particles and decreases with increasing wavelengths, superimposed by effects of the variable refractive index as shown in Figure 2c. It is interesting to note that the asymmetry factor may be altered if non spherical particles are considered due to the enhanced sideward scattering (Koepke and Hess, 1988). However this effect depends strongly on the particle radius (Mugnai and Wiscombe, 1986) and thus is not considered in this paper.

4.1 Water-insoluble component

That part of the aerosol particles under mid-latitude conditions which is insoluble in water, is given as component INSO. Its size distribution and refractive index are taken from the dust-like particles (WMO, 1983), after Shettle and Fenn (1979). The particle density used is $\rho = 2.0$

g/cm^3, somewhat less than that of pure clay minerals (Weast, 1976) and thus in agreement with the assumption, that the particles of this component are a mixture of 'dust' and the insoluble part of the organic material is part of this component, which has a lower density (Sloane, 1984).

Optical properties of individual components are sparse in the literature because it is difficult to measure them independently. From a literature review by Trijonis and Pitchford (Malm et al., 1994) scattering efficiency is found to be 0.6 m^2/g for coarse mass, and 1 m^2/g for soil. This is in agreement with the data for INSO, if the mass is integrated over the complete radius range. The values in the Table 4, however, take into account the cut-off radius [of typical particle counters], with the consequence of higher mass optical efficiencies.

The single scattering albedo for INSO indicates relatively high absorption properties. These result from the refractive index used and can be explained with Fe_2O_3 associated with aerosol forming soil, which is highly absorbing (Bohren and Huffman, 1983). Moreover, also the organic material which is not taken into account as soot but as part of INSO may partly be light absorbing carbon (Malm et al., 1994).

4.2 Water-soluble component

The water-soluble part of aerosol particles, which consist of various kinds of sulfates, nitrates and other water soluble substances (Shettle and Fenn, 1979; Shaw and Paur, 1983; Heintzenberg, 1989) is combined to the component WASO the mass of which is about twice that of the mass of sulfate alone. It is assumed to be an internal mixture of all condensable material, as ultimate stage of an aged sub-micrometer particle population. The water-soluble part of the organic material which is assumed to be half of its mass (Jaenicke, 1988; Malm et al., 1994) is also taken to be part of WASO. The component is the dominant part in continental aerosols, but is also used to model the fraction of small aerosols over oceans (Clarke, 1988).

The size distribution of WASO is taken from Shettle and Fenn (1979) which was accepted in WMO (1983), however taking into account that the mode radius which is given there is valid for moderate humidity. To get the radius for dry particles of WASO (Table 1) we calculated their humidity dependency as mentioned under assumption of pure ammonium sulfate and fixed the mode radius in such a way, that the value from Shettle and Fenn (1979) is reached at 75% relative humidity. The particle density used for the dry particles is $\rho = 1.8$ g/cm^3 (Volz, 1972; Weast, 1976).

The refractive index for dry particles is taken from Shettle and Fenn (1979), is primarily based on the measurements of Volz (1972). It describes the component WASO to be slightly absorbing (Table 4) which can be explained by its mixture of different material including parts of organic carbon. The mass scattering efficiency of WASO (Figure 4) is in good agreement with values measured for sulfate particles (Hegg et al., 1993) and assumed to be valid for sulfates, nitrates and organic carbon (Malm et al., 1994) which are the dominant constituents of WASO. This is not valid for scattering of total fine particles (Waggoner and Weiß, 1980). If however, the mass of sulfate only used to describe the scattering coefficient of all scattering particles the mass scattering efficiency is about a factor of two higher (Charlson et al., 1991; Hegg et al., 1993), because the sulfate mass is only about half of the total mass of the scattering particles.

4.3 Soot component

The component called SOOT is used to represent absorbing black carbon particles characterised by its high imaginary part of the refractive index as illustrated in Figure 1. Depending on the way the soot particles are generated and may react during their lifetime in the atmosphere, they have different properties, e.g. different values of the complex refractive index (see Colbeck et al., 1989; Horvath, 1993). The values used are taken from Shettle and Fenn (1979) and are well within the variability found in the literature (see review by Colbeck et al. 1989, Horvath, 1993, Twitty and Weinmann, 1971). As a consequence of the concept of external mixture of components, no internal mixture of soot with hygroscopic particles is assumed. Thus, the size of the soot particles is not varied with relative humidity (Dlugi, 1989). Although aged soot particles are fractal clusters i.e. agglomerations of small, approximately spherical elements strung out in long, often multi-connected chains (Bruce et al., 1991), their radiative properties are thought to be calculated with Mie-theory. Thus, the particles are described as spheres which describes the elements of the chains with a size distribution (Table 1) is taken from WMO (1983). The effects of close vicinity of the particles are neglected, which is possible, because the spheres in the agglomerate act essentially as independent absorbers (Colbeck et al., 1989). Due to the structure with empty space, with high aerodynamic radii, a particle density of 1 g/cm^3 is assumed (Horvath, 1993; Nyeki and Colbeck, 1994).

Experimentally determined values of mass extinction efficiency show the continuous decrease with wavelength (Bruce et al., 1991) which can be seen in Figure 2a for SOOT. The

agreement of single scattering albedo and mass absorption efficiency from Figure 2 and Table 4 with measured values is good (Bruce et al., 1991; Colbeck et al., 1989; Clarke et al., 1987; Gerber and Hindman, 1982; Sloane et al., 1991). But it must be mentioned, that the data in the literature show a variability in the order of two due to the different methods and analysed material.

4.4 Sea-salt components

Sea-salt particles are described with two components which have the same refractive index but are different in size (accumulation mode SSAM and coarse mode SSCM). The size distribution parameters are taken after WMO (1983), where the values are valid for average humidity conditions. Under the assumption, that the r_m given there are valid for a relative humidity of about 75%. The radii for dry particles (Table 1) and for different relative humidities (Table 2), are modelled after Hänel and Zankl (1979).

The refractive index for dry particles is taken from Shettle and Fenn (1979). The density of the dry sea-salt particles is assumed to be $\rho = 2.2$ g/cm^3 (Weast, 1976; Hänel, 1976). Radiative properties will be discussed later for maritime aerosol mixtures.

4.5 Mineral components

Mineral aerosol or desert dust produced in arid regions consists of quartz and clay minerals e.g. hematite. These particles are described by four components, which are assumed to have the same refractive index, but are different in size. Nucleus mode (MINM) accumulation mode (MIAM) and coarse mode (MICM) together with a certain amount of WASO form the aerosols over deserts. A component called mineral transported (MITR) is used to describe the aerosol far away from its sources, transported over long distances, with a reduced amount of large particles, as for example in the Saharan aerosol layer over the Atlantic.

The size distribution parameters of the components which are used to describe the aerosol over deserts are given by d'Almeida (1989) [which are an improved description of his earlier measurements (d'Almeida, 1987)]. Only one set of mineral components is used because additional components give no improvements with respect to the range of variability, which is found when different measurements (from elsewhere than the Sahara) are compared (Patterson and Gilette, 1977; Levin and Lindberg, 1979; d'Almeida and Schütz, 1983; Désalmand et al., 1986; Fouquart et al., 1987; Tanré et al., 1988; Nakajima et al., 1989). The size distribution of the long range transported mineral component is given after Schütz (1979) which fits with

data measured by Kondratyev (1981) and d'Almeida and Schütz (1983). For this component, the radius range is reduced to $0.02 \leq r \leq 5$ µm, to consider the long time, which has passed by the transport of the aerosol particles far away from their sources. That means, in calculation both of mass and of optical properties, the radius range is restricted to these values.

The mineral particles do not change their properties with relative humidity. Their density is $\rho = 2.6$ g/cm^3, which is valid for a mixture of quartz and clay minerals (Weast, 1976) and usually adopted.

The refractive index used is based on a compilation of various data as discussed by Carlson and Benjamin (1980) and Sokolik et al. (1993). The data used are based mainly on Volz (1973), Levin et al. (1980), and Patterson et al. (1977), slightly modified in infrared to take into account quartz absorption features in agreement with transmission measurements (Schütz, 1979).

Nakajima et al. (1989) found optical properties of desert dust, which may result from strong non-sphericity of the particles at least of large particles. However, at present in GADS mineral dust particles are treated to be spherical. This is justified by measurements of Kaufman et al. (1994) and Sokolik and Golitsyn (1992) and by the fact that optical properties calculated with Mie-theory and used for remote sensing purposes lead to results which are in agreement with surface based measurements (Jankowiak and Tanré, 1989; Rao et al., 1988).

Optical properties of desert dust are measured usually for the particle mixture and not for individual components. Thus, they will be discussed later. However, as a first approximation, values measured at high dust load can be compared with that of the accumulation mode, which dominants the optical properties. From Figure 2 the typical spectral behaviour of the extinction coefficient can be seen which is nearly independent of the wavelength in the solar spectral range (Levin et al., 1980; Tanré et al., 1988; Pachenko et al., 1993). For the Sahara aerosol layer, which values have to be compared with MITR $\sigma_e^* = 0.25$ m^2/g was measured by Carlson and Caverly (1977) and $\omega_0 = 0.73$ at 0.5 µm wavelength.

4.6 Sulfate solution

The component called sulfate solution (SUSO) is used to describe stratospheric aerosol and to describe sulfate particles which are found in the Antarctic aerosol and are assumed to have their source in the stratosphere. It is described with size distribution parameters after Shaw (1979) which similarly were found by Yamato et al. (1987). Under the assumption that these particles are 75% H_2SO_4, the refractive index is taken from Fenn et al. (1985) based on the

measurements of Palmer and Williams (1975) and Remsberg (1971 and 1973). The density ρ = 1.7 g/cm^3 is taken from Roth and Scheel (1923).

4.7 Water

Water is not a component itself, but used to describe humidity dependent size changes. This has consequences on particle density and refractive index, which are calculated for humid particles under the assumption of volume additivity. The refractive index of water is given after Shettle and Fenn (1979) on the basis of Hale and Querry (1973).

5 Global distributions of the aerosol components

The global aerosol distribution is given as climatologically averaged values both for the winter (December through February) and summer (June through August) seasons on a global grid with a resolution of 5° by 5° longitude and latitude, independently for the components discussed above. The data are presented as global maps of the aerosol in the first layer above the surface for selected season. The resulting optical properties are discussed in section 7.

In any case, only the dominant components are taken into consideration. That means, in contrast to the results of transport models, aerosol components are neglected, if their amount is very low and if the possible contribution to the radiation budget or climate effects is negligible. The number of components are restricted to at most four which are dominant at each grid cell.

In principle, the presented global maps of aerosol components have been obtained through estimates and analysis of a large number of different measurements and model simulations. Unfortunately, many of measurement methods are not comparable or the measure ranges are not identical. Because the aerosol distribution is temporally and spatially varied in its dependence on formation and removal processes, we have tried to assume an objective analysis on the global scale. For this purpose we have included global fields of meteorological and climatological parameters such as wind, cloud cover and precipitation, as well as the industrial production, surface structure and population. In regions where little or no data are available, the presented aerosol concentration has been identified with other regions which are comparable to these environmental conditions. While this method is not completely satisfactory, it provides an initial attempt to quantify the global aerosol pattern.

The data in GADS are given as number concentration, because the aerosol number concentration can be treated as constant with changes in the relative humidity whereas the mass concentration would change because of the accretion or evaporation of water. However, in the figures to show the global data which follow, we present the distribution of the components as mass concentration, because these data are more meaningful, e.g. with respect to source budgets and can be compared more easily with measurements. However, with respect to measurements, again the effect of cut off must be mentioned, which is taken in following as a 15 µm diameter. The relative humidity used for the figures is taken to be 50 %, with respect to filter measurements with analyse under laboratory conditions.

5.1 Global Field of the component INSO

The component INSO describes water-insoluble aerosol particles from continental, but not desert origin. Figure 3 shows the global distribution of the mass concentration of INSO in the surface layer for the northern winter (December to February). The particles are concentrated near their sources because of the relative short life time of the particles. The sources for insoluble particles are industrial processes, ash, dust from fields and streets, and material from biogenic sources like pollen, spores and leaf litter. Thus the values are highest over dry surfaces with low plant cover (Mishra, 1988). Also, higher mass mixing of water-insoluble particles are found in regions with agriculture and human activities (Heintzenberg, 1989; Malm et al., 1994). Lower values are over woods (Artaxo et al., 1990), and even lower over dense and low plants, at least for wet conditions. The concentration of INSO from natural sources is lower in winter than in summer (Hofmann, 1993; Malm et al., 1994) and lowest over snow. This explains the distribution over the continents, the low values over polar regions, and the differences between summer (not presented here) and winter. In remote regions over oceans, INSO is neglected due to the low values (Gaudichet et al., 1989) and is also neglected in the regions of extended deserts, where mineral particles are used to describe the non-soluble fraction of aerosol.

5.2 Distribution of the component WASO

The component WASO is used to describe water-soluble particles, generated from gas-to-particle conversion, from industrial and natural processes, and also directly emitted water soluble particles from the soil or biological sources. The pattern of WASO which can be seen in Figure 4 results from different sources and sinks which are discussed in the following. The

anthropogenic sources which give the dominant part lead to high mixing ratios over industrial and urban regions (Heintzenberg, 1989; Hänel, 1994) which of course are smoothed out in the geographical resolution used and leads to features similar to that modelled for sulfate, but with higher concentration because WASO includes all water-soluble materials and not just sulfate.
The water-soluble aerosol particles, as mixture of material from anthropogenic and natural sources have a maximum during the summer or seasonally effects may be balanced in proportion how the two parts contribute to the total amount of WASO (Husain and Dutkiewiecz, 1990; Willison et al., 1985; Shaw and Paur, 1983; Hofmann, 1993; Trijonis, 1982). Also seasonally different rain probability changes the WASO amount. This is the reason why over tropical rain forests fine aerosol mass is formed to be larger in dry than in wet season (Andreae et al., 1988; Artaco et al., 1990; Talbot et al., 1988). Water-soluble aerosol particles are also present in desert regions (with some percent in mass) (Patterson and Gilette, 1977; Levin and Lindberg, 1979; d'Almeida and Schütz, 1983; Sokolik and Golitsyn, 1992) and may result both from local and remote sources.
Over oceans the description of the fine particle mode using WASO is in agreement with the general finding, that aerosols in these smaller size categories are composed of sulphate material derived from sea-salt, from dimethylsulfide emissions by biological life in the oceans and by anthropogenic sulfate emissions (Meszaros and Vissy, 1974; Charlson et al., 1987; Hoppel and Frick, 1990). O'Dowd and Smith (1993) found evidence that also small aerosols particles consist mostly of sea-salt, but with little wind speed dependence. Thus, the amount of WASO is assumed to be sea salt sulfate together with non-sea-salt sulfate of biological activity in remote areas with values estimated after Clarke et al. (1987), Erickson et al. (1991) and Fitzgerald (1991). Over the northern Atlantic and the western Pacific, WASO is enhanced in regions with continental influence, (Sievering et al., 1989; Whelpdale et al., 1988; Yamato and Tanaka, 1994). In the north polar regions strong differences are found between winter, with enhanced northern transport from anthropogenic polluted areas with an accumulation of particles as Arctic haze (Wendling et al., 1985; Barrie, 1986; Heintzenberg, 1982; Shaw, 1982) and the conditions in summer when the accumulation is less pronounced.

5.3 Global soot distribution

The global pattern of the mass concentration of SOOT is given in Figure 5, here for the northern summer. SOOT is produced by combustion process, i.e. industries, home, heating, traffic, and biomass burning. Thus its amount is highest in densely populated regions at mid-

latitudes during local winter (Heintzenberg, 1989; Horvath, 1993; Ohta and Okita, 1984; Shah et al., 1986; Hänel, 1994; Huanling et al., 1991). The reported concentrations may be misleading because averages are susceptible to the infrequent occurrence of high concentrations in the data sets. Moreover, to take into account the large size of the grid resolution, the values are reduced against most of the data found (Pinnick et al., 1993).

Emissions from the biomass burning in Africa and South America is dominant during the local dry season (Desalmand et al., 1986; Cachier et al., 1985; Andreae et al., 1988; Artaxo et al., 1990). Forest fires in northern regions are less frequent than in tropical regions (Chung, 1984; Cahoon et al., 1994) and this is considered with no soot or very low soot values.

From the northern industrialised regions soot also is transported over the oceans (Ohta and Okita, 1984; O'Dowd et al., 1993) and during the winter months to the Arctic so that the concentration increases (not shown here) (Rosen et al., 1981; Rahn, 1981; Shaw et al., 1993). Soot particles which are transported over the tropical Atlantic and Pacific are neglected because their total amount is low (Andreae et al., 1994; Clarke, 1989).

5.4 Number concentration of sea-salt

Sea-salt particles of oceanic origin are representative for the boundary layer over oceans together with the water-soluble component which was already discussed (Meszaros and Vissy, 1974). The number concentration of the sea-salt particles is mixed from the two sea-salt components SSAM and SSCM which are assumed to be wind speed depended. This is the dominant factor for their amount (Hoppel et al., 1990), although individual scatter plots show that salt mass concentrations can vary by an order of magnitude e.g. due to precipitation which may reduce the concentration (Hoppel and Frick, 1990). The expressions

$$N_{SSAM} = \exp (0.18 \cdot u + 1.4) \qquad (5.1)$$

$$N_{SSCM} = \exp (0.23 \cdot u - 7.8)$$

which relate the particle number concentration to the wind speed u in m/s are developed using data which give number concentrations (Smith et al., 1993; O'Dowd and Smith, 1993), data of mass concentrations (WMO, 1983; Erickson et al., 1986; Marks, 1990; Fitzgerald, 1991) and also fit measured size distributions (Hoppel et al., 1990, Fitzgerald, 1991).

The equations take into account that the increase of particle concentration with increasing wind speed is more pronounced for larger particles (Monahan et al., 1983; Smith et al., 1993). The data also fit values measured at higher levels in the atmosphere (WMO, 1983; Bergametti

et al., 1989) if the height distribution for maritime conditions is taken into account and the wind speed is reduced to that at sea level.

The geographical distribution of sea-salt presented in Figure 6 as number concentration of SSAM for the northern summer is calculated after Equation (5.1) from the wind speed modelled in the climate model ECHAM (Roeckner et al., 1992) as an climatological average for the season in consideration. It is obviously that due to the seasonal variations of the wind velocity the strong difference in high-latitude of northern and southern hemisphere and the tropical region is caused. Sea-salt is part of the polar aerosols (Barrie and Hoff, 1985; Pacyna and Ottar, 1985; Cunningham and Zoller, 1981) and near the coast may be part of continental aerosol (Willson et al., 1985). This is modelled only with the sea-salt accumulation mode, because the larger sea salt particles are not transported over longer distances (Rossknecht et al., 1973).

5.5 Global distribution of mineral particles

The aerosol over deserts is mixed from the three mineral components MINM, MIAM and MICM, together with a certain part of WASO as mentioned above. Impact of salting sand grains is the most important mechanism responsible for dust entrainment. This effect is wind velocity dependent, but its variability is controlled by a combination of saltation energetics and soil mechanisms (Shao et al., 1993). These are soil-dependent factors, with the result that arid regions have higher dust potential than hyper arid regions (Pye, 1989) and that the threshold velocity is highly variable (Nickling and Gillies, 1989). However, in every case was found that with increasing total amount of particles also the relative amount of large particles increases (Mélice et al., 1984; d'Almeida, 1987; Tanré et al., 1988; Nakajima et al., 1989; Schütz et al., 1981). Thus, the mixture of the mineral components to describe the size distribution is not related to the wind speed, but to turbidity, that means to the total amount of mineral particles. On the basis of measured size spectra from different deserts, both number and volume distributions, a correlation was determined between the total number of mineral particles of a desert aerosol, $N_{mineral}$, and the numbers N_i of the three components MINM, MIAM and MICM from Table 1:

$$\begin{aligned} \ln N_{MINM} &\cong 0.104 + 0.963 \ln N_{mineral} \\ \ln N_{MIAM} &\cong -3.94 + 1.29 \ln N_{mineral} \\ \ln N_{MICM} &\cong -13.7 + 2.06 \ln N_{mineral} \end{aligned} \qquad (5.2)$$

Rounding errors in Equation 5.2 exceed 4 % for $N_{mineral} < 20$, which however is not restriction with respect to natural conditions because it corresponds to a visibility of more than 100 km. The approximations in Equation 5.2 are used to describe the size distribution of mineral aerosols at all deserts in the world. The total number of mineral particles is described on the basis of a variety of measurements from optical depth to mass loading, from visibility to dust storm frequency. The component MITR in addition is used to describe desert aerosol transported away from its source in a level above the surface as mentioned in chapter 6, and also to describe mineral aerosol particles in the boundary layer for regions away from the large deserts and for smaller desert regions like Arizona and Namibia.

The amount and geographical distribution of mineral aerosol is different for summer and winter due to different atmospheric circulation. To get the amount of mineral dust over Sahara measurement of number and mass concentration are used, but also data of visibility and optical depth from ground and satellite are considered and converted to concentration in the surface layer taking into account the height distribution presented in chapter 6 (d'Almeida, 1986; d'Almeida and Schütz, 1983; Melice et al., 1984; Joseph et al., 1973; Merill et al., 1989; N'Tchayi et al., 1994; Legrand et al., 1995; Schütz et al., 1981). All types of information, such as dust storm frequency, is used for desert regions outside Sahara where the mineral dust amount is less frequently analysed (Arkawa, 1969; Middleton, 1989; Bergametti et al., 1989; Prospero, 1981; Gao et al., 1992; Golitsyn and Gillette, 1993; Goudie and Middleton, 1992; Isakov et al., 1992; Merrill et al., 1989). Observations from ground, aircraft and satellite are taken to describe the distribution of the mineral aerosol transported from the Sahara over the Atlantic (Prospero and Carlson, 1972; Talbot et al., 1986; Swap et al., 1992), and Mediterranean (Dulac et al., 1992) and from the Gobi desert over China to the Pacific (Merrill et al., 1989; Zhang et al., 1993).

The total mass concentration of all mineral components is combined in Figure 7, as example for winter. Both the mineral mass in the surface layer is presented with green over yellow to red colouring, and the mineral aerosol mass in the higher levels where it is transported signed by blue colour. Corresponding to this global winter distribution the summer field is globally similar however the far transport over the Atlantic drifts approximately 10 degrees northwards.

5.6 Distribution of SUSO

The component SUSO not shown in a Figure is used to describe the sulfate aerosols in the Antarctic region (Shaw, 1979; Ito, 1993) with increased values in the southern summer (Maenhaut et al., 1979; Cunningham and Zoller, 1981).

6 Vertical aerosol distribution

Vertical distribution of aerosols in the troposphere is highly variable (Reagan et al., 1984; Sasano and Browell, 1989; Kristament et al., 1993) depending at least on the actual thermal structure and on vertical mixing processes and thus on actual weather, season, time during the day and properties of underlying surface. However, here due to the general averaging, on the one hand, and the limited possibility of vertical resolution in climate models, on the other hand, only a simple description of vertical aerosol distribution is taken into account. Moreover, the height distribution of each grid point is assumed to be independent of season. The atmosphere is separated into a boundary layer, the free troposphere and the stratosphere. For each gridpoint the aerosol properties within these layers are not modified in composition but in their amount. In cases with transported desert dust in an upper level, an additional layer is inserted between the boundary layer and the free troposphere.

Within the boundary layer the aerosol is well mixed and the mixing ratio of the aerosol components presented previously is assumed constant in the layer. The depth of the boundary layer depends mainly on the underlying surface, on the season and on the aerosol formation processes in the approximate range of 1 to 6 km above the ground.

Over land surfaces outside deserts a constant mixing in a layer with height is assumed, in a boundary layer of 2 km (WMO, 1983; Pinnick et al., 1993). Over oceans, convection and thus mixing of aerosol with height is less pronounced, resulting in an exponential decrease with a scale height of 1 km in the boundary layer of 2 km height (Patterson et al., 1980; Kristament et al., 1993). In cases with an additional dust layer above, this is settled between 2 km and 3.5 km, with a concentration independent with height (Prospero and Carlson, 1972; Schütz et al., 1981). Over deserts, the lifting of aerosol particles reaches higher levels, that is the layer with desert aerosol is 6 km with an exponential decrease with a scale height of 2 km (Jaenicke, 1992). In the Arctic in winter an aerosol layer is found well above the ground, with concentrations which may be higher at higher levels (Barrie, 1986; Pacyna and Ottar, 1988;

Heintzenberg et al., 1991) because the aerosol sources are mainly outside the region. This behaviour is described by the boundary layer up to ~ 2 km with a particle concentration which is taken as fixed with height. In the Antarctic region, outside the area near the shore, down-welling results in a good mixture of aerosol with air molecules (Tomoyuki, 1989; Ito, 1989) over the total layer, which is assumed to be ~ 5 km height with respect to the elevated surface.

Above the boundary layer the free tropospheric aerosol is described for regions north of 20°N by an aged continental aerosol (Kent et al, 1991; Heintzenberg et al., 1991; Clarke, 1992), even over the oceans (Patterson et al. 1980), because it is mainly due to thermal transports over land (Davies, 1987) and thus mixed by components of WASO, SOOT and INSO. For the equatorial region and the southern hemisphere it is modelled by the water-soluble component alone.

The concentration of the free tropospheric aerosol is varied with respect to geographical latitude and season on the basis of satellite observations (Kent et al., 1991). The layer with free tropospheric aerosol is modelled with constant mixing, i.e. a scale height of about 8 km from the top of the boundary layer or from above the layer with transported mineral aerosol up to 12 km, which is used as a fixed value for the height of the tropopause.

The tropopause height as well as the amount of stratospheric aerosol is not varied, because the present study is focused on the tropospheric aerosol. But, for the purpose calculating the total optical depth, values for the stratospheric aerosol is described by the aerosol component SUSO with fixed non-volcanic value (Schult, 1992). For use in GCM in general a more detailed stratospheric aerosol climatology, such as developed by McCormick and Wang (1993) should be used. After many major volcanic eruptions there is a significant increase in the stratospheric aerosol loading for upwards of three years afterwards. For such cases higher particle concentrations must be used based on values measured or modelled as a function of time after the eruption, (e.g. Sato et al., 1993).

The profiles of the number distribution can directly be used to describe height distribution of optical quantities related to particle concentration. The specific profiles described above are not varied with aerosol components or local environmental conditions like rain or clouds, due to the sparse number of investigations. They also are not correlated to geographic latitude and season or properties of surface. However, such a connection is feasible due to the variation of convective processes and should be added in a later version of GADS.

7 Global distribution of aerosol related properties

In this section we present properties of the aerosol externally mixed from its components based on the GADS. Both for winter and summer global maps are presented properties like of mass concentration and optical depth, which easily can be compared with measurements.

7.1 Mass concentration of the mixed components

The total mass concentration of the combined external mixture of the aerosols is equal to the sum of the individual aerosol components with the global distributions as described in the previous section. Figure 8 shows the mass concentration of the mixed aerosols in the surface layer both for the northern winter (Figure 8a) and for summer (Figure 8b). Mineral aerosols lifted by convection to elevated levels, and transported, in a second aerosol layer are not included in this data. The presented data are based on the assumption of the relative humidity of 50% and a maximum measured radius of 7.5 μm. The highest mass concentration, in the order of 400 $\mu g/m^3$ occurs over the Sahara desert where heavy mineral particles are the predominant sources.

Further remarkable in Figure 8 is the high mass concentration over oceans. Aerosols of oceanic origin are largely sea-salt particles which together with a background water-soluble aerosol, is representative for the boundary layer over oceans. Thus, maritime aerosol is mixed from the two sea-salt components SSAM and SSCM, together with WASO and, at places which are influenced by land or anthropogenic aerosols, SOOT and INSO are added. Due to the higher wind speeds in the winter and the associated with a higher sea-salt input compared with the summer, the mass concentration reaches values up to 50 $\mu g/m^3$ over the northern hemisphere oceans. The Figure also includes the long range transport of aerosol over the northern Atlantic from industrial production.

Atmospheric aerosol over continental regions outside deserts usually is a mixture of gas-to-particle and bulk-to-particle aerosols and thus a mixture of the insoluble and water-soluble components, with the potentiality of soot. The mass concentration amounts to in the range of 10 up to 40 $\mu g/m^3$ which is in agreement with observations. In the region of the influence of an ocean, sea-salt may be part of continental aerosol. This is modelled only with the sea-salt accumulation mode, because the larger sea salt particles are not transported over longer distances. Likewise, near deserts mineral components may be part of the continental aerosol.

As indicated in Figure 8, the mass concentration of aerosol is small over polar regions. Arctic aerosols, i.e. the aerosol over the snow and ice covered areas, are mixed from INSO, WASO, SOOT and SSAM (Shaw, 1982; Clarke et al., 1984; Barrie, 1986; Clarke, 1989; O'Dowd and Smith, 1993), with differing mixtures for the winter and summer conditions.

The aerosol for the Antarctic region is described as mixed from sulphate (SUSO) together with sea-salt (SSAM) and a mineral component (MITR) with mixing ratios after Shaw (1979) and Cunningham and Zoller (1981). The amount of particles is increased compared to that at the pole station (Artaxo et al., 1992; Guerzoni et al., 1992), because the data are not varied over the total Antarctic continent due to limited knowledge.

7.2 Optical depth of total aerosol

In Figure 9 the optical depth are presented for relative humidity of 50%, as an representative average for the lower troposphere. The relative humidity is not varied with season and location in the figure, to show the effect of spatial variations of the aerosol loading and not of the humidity variations. Shown are maps of the optical depth at 0.5 μm wavelength which is given, on the one hand to compare with satellite observations, and on the other hand, to present the radiative aerosol effect integrated over solar spectral range, which together with the surface albedo and solar elevation is most relevant for aerosol direct climate forcing. This optical value is given to show the high variability of this quantity, even over continental surfaces.

The optical depth is high over high polluted regions of the northern hemisphere, and a bit higher in summer. Since the wind speed over the ocean varies with the season and geographical location, the resultant optical depth over oceans also varies and is within the range of 0.05 to 0.18 which is well in accordance with seasonal maps by polar orbiting satellites after Husar et al. (1995).

High optical depths have been found over deserts as well as over tropical Atlantic caused by the long range transport of mineral particles. The area of higher optical depth over Atlantic mainly produced by this long range transport and represented by the MITR, is located more northerly in the summer than in the winter due to the changed circulation. Again, it can be seen, that the values in the GADS show the good agreement with the data usually found in the literature (e.g. Kaufman, 1995).

For the interpretation and comparison of the results we use the zonal mean values, although it should be noted that the global patterns are highly variable. Figure 10 shows the zonally

averaged optical depth at a wave length of 0.5 μm and a assumed relative humidity of 50% for the total aerosol loading within the atmosphere and the contribution thereof from the land and ocean for winter and summer, respectively. The peak zonal mean optical depth occurs over the tropical latitudes, and is dominated by the contribution from desert aerosol which alone gives a zonal mean optical depth of 0.32 for winter and of 0.28 for summer. Also as expected the optical depth is high over the main anthropogenic source region of northern hemisphere mid-latitudes and over the ocean in the high wind speed region of the south hemisphere.

The global annual mean optical by total aerosols is resulted of 0.101 at 50% relative humidity. Note, that the optical depth for differently assumed humidities is significantly distinguished, with a global mean of 0.063 for 0% compared to 0.139 for 80% in winter. Thus an increase in the relative humidity leads to an increase in the optical depth, especially over ocean where the relative humidity is often much higher than 50%.

8 Conclusion

The Global Aerosol Data Set presented here is a new data compilation in which the current aerosol measurements and model results have been included. The global distribution of atmospheric aerosols has been described in terms of the distributions of a set of ten principal aerosol types. These aerosol components have been selected and defined through their particle size distribution and their wavelength dependent index of refraction. For these components, the normalised optical parameters are calculated using Mie scattering theory. Additionally, the global fields of the mixture of aerosol components are defined, including their vertical profiles, for winter and summer.

In 1983, the conclusion of an experts' meeting on aerosols (WMO, 1983) was: that because of the large spatial and temporal variability of aerosols in the atmosphere, especially in the troposphere, it was not possible with the then existing techniques to make sufficient measurements to give statistical means and variances of aerosol properties which are suitable for climate modelling. Since that time measurement techniques have been improved, however the amount of measured data is still too low for satisfactory statistical means, and other significant uncertainties still remain (Charlson and Heintzenberg, 1995).

These are uncertainties with respect to:

- quality of the basic measurements which are limited in time and places
- incompleteness of measurements (insufficient closure experiments)

- description of aerosol particles with a limited number of components
- quality of the data (refractive index and size distribution) to describe the components
- validity of mixture and amount of components to give aerosol as an average for a specific location
- aerosol height distribution
- aerosol description at places without measurements
- calculation of radiative properties with Mie-theory which neglects non-sphericity of particles.

In this sense, the Global Aerosol Data Set presented here is of limited nature. However, it should be mentioned, that the brick-box principle easily allows to improve the data, especially by improved properties of individual components, the aerosol height profiles and the global distribution or another scatter code instead of Mie-theory. Furthermore, if temporal changes of the aerosol properties on a global scale should be present, or a trend of aerosols is observed it would be possible to integrate changes due into the physical definition of the data set.

With respect to the limited nature of the data, recommendations on overlooked data, on new measurements or other suggestions for improvements would be highly appreciated by the authors. In addition, during the next several years a number of new satellite measurements will be making measurements of the tropospheric aerosols and their radiative properties both over the ocean and over land (e.g. MODIS, MISR, MOS, MEKIS, POLDER). Also the results from several major aerosol field measurement campaigns [ACE-1 and TARFOX] are currently being analyzed, or are about to take place, [ACE-2]. As the new data become available it will be necessary to modify the components of the GADS and their global distribution.

By now, the GADS is a basis for appraising direct radiative forcing by aerosols, with the right order of magnitude, and with spatial resolution which allows to include effects of albedo and sun position. Extensive investigations of climate effects by atmospheric aerosols based on this GADS have been started.

Acknowledgements

We want to thank to G.A. d'Almeida for the work he did on the development of the first version of the aerosol climatology which was used as the basis for GADS. We would like to thank György Hermann for his help in programming

References

Andreae, M.O., B.E. Anderson, D.R. Blake, J.D. Bradshaw, J.E. Collins, G.L. Gregory, G.W. Sachse, and M.C. Shipham, 1994: Influence of plumes from biomass burning on atmospheric chemistry over the equatorial and tropical South Atlantic during CITE3. *J. Geophys. Res.*, 99, 6, 12.793-12.808.

Andreae, M.O., E.V. Browell, M. Garstang, G.L. Gregory, R.C. Harriss, G.F. Hill, D.J. Jacob, M.C. Pereira, G.W. Sachse, A.W. Setzer, P.L. Silva Dias, R.W. Talbot, A.L. Torres, and S.C. Wofsy, 1988: Biomass-burning emissions and associated haze layers over amazonia. *J. Geophys. Res.*, 93, 1509-1527.

Arkawa, H. (Ed.), 1969: *Climates of northern and eastern Asia.* Elsevir Pub. Comp., Amsterdam. p. 6-86.

Artaxo, P., M.L.C. Rabello, W. Maenhant, and R. van Grieben, 1992: Trace elements and individual particle analysis of atmospheric aerosols from the Antartic peninsula. *Tellus*, 44B, 318-340.

Artaxo, P., W. Maenhaut, H. Storms, and R. v. Grieken, 1990: Aerosol characteristics and sources for the amazon basin during the wet season. *J. Geophys. Res.*, 95, D10 16.971-16.985.

Barrie, L.A., 1986: Arctic air pollution: an overview of current knowledge. *Atmos. Environ.*, 20, 643-663.

Barrie, L.A. and R.M. Hoff, 1985: Five years of air chemistry observations in the canadian arctic. *Atmos. Environ.*, 19, 1995-2010.

Bashurova, V.S., V. Dreiling, T.V. Hodger, R. Jaenicke, K.P. Koutsenogii, P.K. Koutsenogii, M. Kraemer, V.I. Makarov, V.A. Obolkin, V.L. Potjomkin, and A.Y. Puseb, 1992: Measurements of atmospheric condensation nuclei size distributions in Siberia. *J. Aerosol. Sci.*, 23, 191-199.

Bergametti, G., A.L. Dutot, P. Buat-Ménard, R. Losno, and E. Remoudaki, 1989: Seasonal variability of the elemental composition of atmospheric aerosol particles over the northwestern Mediterranean. *Tellus*, 41B, 353-361.

Bohren, C.F. and D.R. Huffmann, 1983: *Absorption and scattering of light by small particles.* Wiley Interscience, New York.

Bruce, Ch.W., Th.F. Stromberg, K.P. Gurton and J.B. Mozer, 1991: Trans-spectral absorption and scattering of electromagnetic radiation by diesel soot. *Appl. Opt.*, 30, 1537-1546.

Cachier, H., P. Buat-Menard, M. Fontugne, 1985: Source terms and source strengths of the carbonaceous aerosol in the tropics. J. *Atmos. Chem.*, 3, 469-489.

Cahoon, D.R., B.J. Stocks, J.S. Levine, W.R. Cofer, and J.M. Pierson, 1994: Satellite analysis of the severe 1987 forest fires in northern China and southeastern Siberia. J. *Geophys. Res.*, 99, 9, 18.627-18.638.

Carlson, T.N. and R.S. Caverly (1977: Radiative characteristics of saharan dust at solar wavelengths. *J. Geophys. Res.*, 82, 3141-3152.

Carlson, T.N. and St.G. Benjamin, 1980: Radiative heating rates for saharan dust. *J. Atmos. Sc.*, 193-213.

Charlson, R. J., and J. Heintzenberg, (Eds.), 1995: *Aerosol forcing and climate*, Dahlem Workshop Reports, Environm. Sci. Res. Report 17, John Wiley & Sons, 416 pp.

Charlson, R.J. J.E. Lovelock, M.O. Andreae, and St.G. Warren, 1987: Oceanic phytoplankton, atmospheric sulphur, cloud albedo and climate. *Nature*, 326, 655-661.

Charlson, R.J., J. Langner, H. Rodhe, C.B. Leovy and S.G. Warren, 1991: Perturbation of the northern hemisphere radiative balance by backscattering from anthropogenic sulfate aerosols. *Tellus*, 43AB, 152-163.

Charlson, R.J., S.E. Schwartz, J.M. Hales, R.D. Cess, J.A. Coakley, Jr., J.E. Hansen, and D.J. Hofmann, 1992: Climate forcing by anthropogenic aerosols. *Science*, 255, 423-430.

Chung, Y.-S., 1984: On the forest fires and the analysis of air quality data and total atmospheric ozone. *Atmos. Environ.*, 18, 2153-2157.

Clarke A.D., 1988: Aerosol physical chemistry in remote marine regions. *J. Aerosol Sci.*, 19, 7, 1195-1198

Clarke, A.D., 1989: Aerosol Light Absorption by Soot in Remote Environments. *Aerosols Sci. Tech.* 10, 161-171.

Clarke, A.D., 1992: Atmospheric Nuclei in the Remote Free-Troposphere. *J. Atmos. Chem.*, 14, 479-488.

Clarke, A.D., K.J. Noone, J. Heintzenberg, St.G. Warren, and D.S. Covert, 1987: Aerosol light absorption measurement techniques: analysis and intercomparisons. *Atmos. Environ.*, 21, 1455-1465.

Clarke, A.D., N.C. Ahlquist and D.S. Covert, 1987: The Pacific marine aerosol: Evidence for natural acid sulfates. *J. Geophys. Res.*, Vol. 92, D4, 4179-4190.

Clarke, A.D., R.J. Charlson and L.F. Radke, 1984: Airborne observations of artic aerosol, IV: Optical Properties of Arctic Haze. *Geophys. Res. Lett.*, 11, 405-408.

Colbeck, I., E.J. Hardman and R.M. Harrison, 1989: Optical and dynamical properties of fractal clusters of carbonaceous smoke. *J. Aerosol Sci.*, 30, 765-774.

Coude-Gaussen, G.P. Rognon, G. Bergametti, L. Gomes, B. Strauss, J.M. Gros amd M.N. LeCoustumer, 1987: Saharan dust on Fuerteventura island (Canaries): chemical and mineralogical characteristics, air mass trajectories, and probable sources. *J. Geophys. Res.*, 92, D8, 9753-9771.

Cunningham, W.C. and W.H. Zoller, 1981: The chemical composition of remote area aerosols. *J. Aerosol Sci.*, 12, 367-384.

d'Almeida, G.A., 1986: A model for saharan dust transport. *Am. Meteor. Soc.*, 25, 903-916.

d'Almeida, G.A., 1987: On the Variability of Desert Aerosol Radiative Characteristics. *J. Geophys. Res.*, 92, D3, 3017-3026.

d'Almeida, G.A., 1989: Desert aerosol: characteristics and effects on climate. in: M. Leinen and M. Sarnthein (eds.), *Paleoclimatology and Paleometeorology: Modern and Past Patters of Global Atmospheric Transport*, 311-338.

d'Almeida, G.A. and L. Schütz, 1983: Number, mass and volume distributions of mineral aerosol and soils of the Sahara. *J. Clim. Appl. Meteorol.*, 25, 903-916.

d'Almeida, G.A., P. Koepke, and E.P. Shettle, 1991: *Atmospheric aerosols: global climatology and radiative characteristics.* A. Deepak Publ. Hampton, Vi., 557 pp.

Davies, C.N., 1987: Particles in the atmosphere: A review. *J. Aerosol. Sci.*, 18, 469-477.

Dekker, H. and G. deLeeuw, 1993: Bubble excitation of surfacde waves and aerosol droplet production: a simple dynamical model. *J. Geophys. Res.*, 98, C6, 10.223-10.132.

Désalmand, F., R. Serpolay and J. Podzimek, 1986: General features of the aerosol observed in the guinean savannah at the level of the ITCZ; influence of the drought. *J. Aerosol Sci.*, 17, 149-156.

Dlugi, R., 1989: Chemistry and deposition of soot particles in moist air and fog. *Aerosol Sci. Tech.*, 10, 93-105.

Dulac, F., D. Tanré, G. Bergametti, P. Buat-Ménard, M. Desbois and D. Sutton, 1992: Assessment of the African airborne dust over the western Mediterranean Sea using Meteosat data. *J. Geophs. Res.*, 97, D2, 2489-2506.

Erickson, D.J., J.J. Walton, S.J. Ghan, and J.E. Penner, 1991: Three-dimensional modeling of the global atmospheric sulfur cycle: a first step. *Atmos. Environ.*, 25A, 513-2520.

Fenn, R.W., S.A. Clough, W.O.Gallery, R.E. Good, F.X.Kneizys, J.D. Mill, L.S. Rothman, E.P. Shettle, and F.E. Volz, 1985: "Optical and Infrared Properties of the Atmosphere", Chap. 18 in *Handbook of Geophysics and the Space Environment*, ed. by A.S. Jursa, Air Force Geophysics Laboratory, Hanscom AFB MA.

Fitzgerald, J.W., 1991: Marine aerosols: a review., *Atmos. Environ.*, 25A, 533-545.

Fouquart, Y., B. Bonnel, M. Ch. Roquai, R. Santer, and A. Cerf, 1987: Observations of saharan aerosols: results of eclats field experiment. part II: broadband radiative characteristics of the aerosols and vertical radiative flux divergence. *J. Clim. Appl. Meteor.*, 26, 28-37.

Gao, Y., R. Arimoto, R.A. Duce, D.S. Lee and M.Y. Zhou, 1992: Input of atmospheric trace elements and mineral matter to the yellow sea during the spring of a low-dust year. *J. Geophys. Res.* 97, 4, 3767-3777.

Gaudichet, A., R. Lefèvre, A. Gaudry, B. Ardouin, G. Lambert and J.M. Miller, 1989: Mineralogical composition of aerosols at Amsterdam Island. *Tellus*, 41B, 344-352.

Gerber, H.E., E. Hindmann (Eds.), 1982: *Light absorption by aerosol particles.* Spectrum Press, Hampotn, Vi., p. 391.

Golitsyn, G., and D.A. Gilette, 1993: Introduction: A joint Soviet-American experiment for the study of Asian desert dust and its impact on local meteorological conditions and climate. *Atmos. Environ.*, 27A, 2467-2470.

Goudie, A.S., and N.J. Middleton, 1992: The changing frequency of dust storms through time. *Clim. Change*, 20, 197-225.

Grassl, H., 1988: What are the radiative and climatic consequences of a changing concentration of atmospheric aerosol particles? In: *The Changing Atmosphere*, F.S. Rowland and I.S.A. Isaksen (Eds.), John Wiley & Sons, Chichester, 187-199.

Guerzoni, S., R. Lenaz, G. Quarantotto, M. Taviani, G. Rampazzo, M.L. Facchini, and S. Fuzzi, 1992: Geochemistry of airborne particles from the lower troposphere of Terra Nova Bay, Antarctica. *Tellus*, 44B, 304-310.

Hale, G.M., and M.R. Querry, 1973: Optical constants of water in the 200-nm to 200-mm wavelength region. *Appl. Opt.*, 12, 555-563.

Hänel, G., 1976: The properties of atmospheric aerosol particles as functions of the relative humidity at thermodynamic equilibrium with the surrounding moist air. *Adv. Geophys.*, 19, 73-188.

Hänel, G., 1994: Optical properties of atmospheric particles: complete parameter sets obtained through polar photometry and an improved inversion technique. *Appl. Opt.*, 33, 7187-7199.

Hänel, G., and B. Zankl, 1979: Aerosol size and relative humidity: Water uptake by a mixture of salt. *Tellus*, 31, 478-486.

Hansen, J., 1993: Climate Forcing and Feedbacks. In: J. Hansen, W. Rossow, and I. Fung (Eds.), *Long-term monitoring of global climate forcings and feedbacks.* NASA Conf. Publ. 3234, pp. 6-12.

Hansen, J.E., and A.A. Lacis, 1990: Sun and dust versus greenhouse gases: An assessment of their relative roles in global climate change. *Nature* 346, 713-719.

Hegg, D.A., R.J. Ferek, and P.V. Hobbs, 1993: aerosol size distribution in the cloudy atmospheric boundary layer of the North Atlantic Ocean. *J. Geophys. Res.*, 98, D5, 8841-8846.

Heintzenberg, J., 1982: Size-Segregated Measurements of Particulate Elemental Carbon and Aerosol Light Absorption at Remote Arctic Locations. *Atmos. Environ.* 16, 2461-2469.

Heintzenberg, J., 1989: Fine particles in the global troposphere. *Tellus*, 41B, 149-160.

Heintzenberg, J., J. Ström, J.A. Ogren and H.-P. Fimpel, 1991: Vertical profiles of aerosol properties in the summer troposphere of central Europe, Scandinavia and the Svalbard region. *Atmos. Environ.*, 25A, 621-627.

Hess, M., P. Koepke, and I. Schult, 1996: Optical properties of aerosols and clouds. the software package OPAC. submitted to *J. Atm. Ocean. Technology.*

Hofmann, D.J., 1993: Twenty years of balloon-borne tropospheric aerosol measurements at Laramie, Wyoming. *J. Geophys. Res.*, 98, D7, 12.753-12.766.

Hoppel, W.A. and G.M. Frick, 1990: Submicron aerosol size distributions measured over the tropical and South Pacific. *Atmos. Environ.*, 24A, 645-659.

Hoppel, W.A., G.M. Frick, and J.W. Fitzgerald, 1994: Marine boundary layer measurements of new particle formation and the effects nonpresipitating clouds have on aerosol size distribution. *J. Geophys. Res.*, 99, 7, 14.443-14.459.

Hoppel, W.A., J.W. Fitzgerald, G.M. Frick, and R.E. Larson, 1990: aerosol size distribution and optical properties found in the marine boundary layer over the Atlantic Ocean. *J. Geophys. Res.* 95, D4, 3659-3686.

Horvath, H., 1993: Atmospheric Light Absorption - A Review. *Atmos. Environ.*, 27A, 293-317.

Hualing, H., X. Jun, and H. Zheng, 1991: The characteristics of imaginary part of aerosol refractive index in some place of Eastern China. *Chinese J. Atm. Sci.*, 15, 230-236.

Husain, L., and V.A. Dutkiewiecz, 1990: A long term (1975-1988) study of atmospheric SO_4: regional contributions and concentration trends. *Atmos. Environ.*, 24A, 1175-1187.

Husar, R.B., L.L. Stowe, and J.M. Prospero, 1996: "Satellite Sensing of Tropospheric Aerosols over the Oceans with AVHRR", submitted to *J. Geophys. Res.*

Isakov, A.A., Nazarov, B.I., M.V. Panchenko, S.M. Pirogov, Ye.V. Romashova, M.A. Sviridenskov, I.N. Sokolik, S.A. Terpugova, Ye.K. Fedorova, Ye.I. Christyakova and A.KH. Shukurov, 1992: The Optical properties of dust plumes. Izvestiya, *Atmospheric and Oceanic Physics*, 28, 8, 607-612.

Ito, T., 1989: Antarctic submicron aerosols and long-range transport of pollutants, Ambio, 18, 34-41.

Ito, T., 1993: Size distribution of Antarctic submicron aerosols. *Tellus*, 45B, 145-159.

Jaenicke, R., 1988: Physical and chemical properties of the air. In: *Numerical Data and Functional Relationships in Science and Technology,* Landolt-Börnstein New sieries, V: Geophysics and Space Research, 4: Meteorology b: (G. Fischer, ed.). Springer, 391-457.

Jaenicke, R., 1992: Vertical distribution of atmospheric aerosols. In: *Nucleation and Atmospheric Aerosols*, N. Fukuta und P.E. Wagner (Hrg.), A. Deepak Publ., 417-425.

Jankowiak, I. and D. Tanré, 1989: Towards a climatology of the Saharan dust events over the atlantic ocean from METEOSAT imagery. in: Lenoble and Geleyn (Eds.), *IRS'88.* A Deepak Publ., 572-574.

Joseph, J.H., A. Manes, D. Ashbel, 1973: Desert aerosols transported by khamsinic depressions and their climatic effects. *J. Appl. Meteor.*, 12, 792-797.

Kaufman, Y.J., 1995: Remote sensing of direct and indirect aerosol forcing. In: *Aerosol forcing of climate,* R.J. Charlson and J. Heintzenberg (Eds.), 297-332. Dahlem Workshop, Environm. Sci. Res. Report 17, John Wiley & Sons Chichester.

Kaufman, Y.J., A. Gitelson, A. Karnieli, E. Ganor, R.S. Fraser, T. Nakajima, S. Mattoo, B.N. Holben, 1994: Size distribution and scattering phase function of aerosol particles retrieved from sky brightness measurements. *J. Geophys. Res.*, 99, 5, 10.341-10.356.

Kent, G.S., M.P. McCormick, S.K. Schaffner, 1991: Global optical climatology of the free tropospheric aerosol from 1.0-mm satellite occultation measurements. *J. Geophys. Res.*, 96, D3, 5249-5267.

Koepke, P. and M. Hess, 1988: Scattering functions of tropospheric aerosols: the effects of nonspherical particles. *Appl.. Opt.*, 27, 12, 2422-2430.

Kondratyev, K.Ya., R.M. Welch, S.K. Cox, V.S. Grishechkin, V.A. Ivanov, M.A. Prokofyev, V.F. Zhvalev and O.B. Vasillyev, 1981: Determination of vertical profiles of aerosol size spectra from aircraft radiative flux measurements. 1. retrieval of spherical particle size distributions. *J. Geophys. Res.*, 86, C10, 9783-9793.

Kristament, I.S., J.B. Liley, and M.J. Harvey, 1993: Aerosol Variability in the Vertical in the Southern Pacific. *J. Geophys. Res.*, 98, D4, 7129-7139.

Lacis, A.A. and M.I. Mishchenko, 1995: Climate forcing, climate sensitivity, and climate response: a radiative modeling perspective on atmospheric aerosols. In: *Aerosol forcing of climate*, R.J. Charlson and J. Heintzenberg (Eds.), Wiley, Chichester, 11-42.

Legrand, M., C. N'doumé and A. Plana, 1995: Saharan dust climatology over North Africa using the IR imagery of Meteosat. submitted *J. Geophys. Res.*

Levin, Z. and J.D. Lindberg, 1979: Sie distribution, chemical composition, and optical properties of urban and desert aerosols in Israel. *J. Geophys. Res.*, 84, C11, 6941-6950.

Levin, Z., J.H. Joseph and Y. Mekler, 1980: Properties of Sharav (Khamsin) dust - comparison of optical and direct sampling data. *J. Atmos. Sci.*, 37, 882-891.

Maenhaut, W., W.H. Zoller, R.A. Duce and G.L. Hoffman, 1979: Concentration and size distribution of particulate trace elements in the south polar atmosphere. *J. Geoph. Res.*, 2421-2431.

Malm, W.C., J.F. Sisler, D. Hoffamnn, R.A. Eldred and Th.A. Cahill, 1994: Spatial and seasonal trends in particle concentration and optical extinction in the United States. *J. Geophys. Res.*, 9, 1, 1347-1370.

Marks, R., 1990: Preliminary investigations on the influence of rain on the production, concentration, and vertical distribution of sea salt aerosol. *J. Geophys. Res.*, 95, C12, 22.299-22.304.

Mélice, J.L., A. Boughanmi, F. Eaton, and G. Wendler, 1984: Turbidity measurements of Saharan aerosol and their effects on atmospheric heating and planetary reflectivity. *Arch. Met. Geoph. Biocl.*, B35, 203-220.

Merrill, J.T., M. Uematsu, and R. Bleck, 1989: Meteorological analysis of long range transport of mineral aerosols over the North Pacific. *J. Geophys. Res.*, 94, D6, 8584-8598.

Mészaros, E. and A. Vissy, 1974: Concentration, size distribution and chemical nature of atmospheric aerosol particles in remote oceanic areas. *J. Aerosol Sci.*, 5, 101-109.

Middelton, N.J., 1989: Climatic controls on the frequency, magnitude and distribution of dust storms; examples from India/Pakistan, Mauritania and Mongolia. In: M. Leinen and M. Sarnthein (eds.), *Paleoclimatology and Paleometeorology: Modern and Past Patters of Global Atmospheric Transport*, 97-132.

Mishra, U.C., 1988: Studies on aerosol size distribution and composition. *J. Aerosol Sci.*, 19, 7, 1165-1169.

Mugnai, A., and W.J. Wiscombe , 1986: Scattering from nonspherical chebyshev particles. 1: Cross sections, single-scattering albedo, asymmetry factor and back scattered fraction. *Appl. Opt.*, 25, 1235-1244.

N'Tchayi, G.M., J. Bertrand, M. Legrand, and J. Baudet, 1994: Temporal and spatial variations of the atmospheric dust loading throughout West Africa over the last thirty years. *Ann. Geophys.*, 12, 265-273.

Nakajima, T., M. Tanaka, M. Yamano, M. Shiobara, K. and Arao, Y. Nakanishi, 1989: Aerosol optical characteristics in the yellow sand events observed in may, 1982 at nagasaki-part II models. *J. Meteor. Soc. Japan*, 67, 2, 279-291.

Nickling, W.G. and J.A. Gillies, 1989: Emission of fine-grained particulates from desert soils. in: M. Leinen and M. Sarnthein (eds.). *Paleoclimatology and Paleometeorology: Modern and Past Patters of Global Atmospheric Transport*, 133-165.

Nyeki, S., and I. Colbeck, 1994: The measurement of the fractal dimension of individual in situ soot agglomerates using a modified millikan cell technique. *J. Aerosol Sci.*, 25, 75-90.

O'Dowd C.D., and M.H. Smith, 1993: Physiochemical properties of aerosols over the northeast atlantic: evidence for wind-speed-related sucmicron sea-salt aerosol production. *J. Geophys. Res.*, D1, 1137-1149.

O'Dowd C.D., M.H. Smith, and S.G. Jennings, 1993: Submicron particle, radon, and soot carbon characteristics over the northeast atlantic. *J. Geophys. Res.*, 98, D1, 1123-1135.

Ohta, S. and T. Okita, 1984: Measurements of particulate carbon in urban and marine air in Japanese areas. *Atmos. Environ.*, 18, 2439-2445.

Pachenko, M.V., S.A. Terpugova, B.A. Bodhaine, A.A. Isakov, M.A. Sviridenkov, I.N. Sokolik, E.V. Romashova, B.I. Nazarov, A.K. Shukurov, E.I. Chistyakova, and T.C. Johnson, 1993: Optical investigations of dust storms during U.S.S.R.-U.S. experiments in Ttadzhikistan, 1989. *Atmos. Environ.*, 27A, 16, 2503-2508.

Pacyna, J.M., and B. Ottar, 1985: Transport and chemical composition of the summer aerosol in the Norwegian Arctic. *Atmos. Environ.*, 19, 2109-2120.

Pacyna, J.M., and B. Ottar, 1988: Vertical distribution of aerosols in the Norwegian Arctic. *Atmos. Environ.*, 22, 2213-2222.

Palmer, K.F. and D. Williams, 1975: Optical constants of sulfuric acid; application to the clouds of venus?. *Appl. Opt.*, 14, 208-219.

Patterson, E.M. and D.A. Gilette, 1977: Commonalities in measured size distributions for aerosols having a soil-derived component. *J. Geophys. Res.*, 82, 15, 2075-2082.

Patterson, E.M., C.S. Kiang, A.C. Delany, A.F. Wartburg, A.C.D. Leslie and B.J. Huebert, 1980: Global measurements of aerosols in remote continental and marine regions: concentrations, size distributions, and optical properties. *J. Geophys. Res.*, 85, C12, 7361-7376.

Patterson, E.M., D.A. Gillete, and B.H. Stockton, 1977: Complex index of refraction between 300 and 700 nm for Saharan aerosols. *J. Geophys. Res.*, 82, 3153-3160.

Penner, J. E., R.J. Charlson, J.M. Hales, N. Laulainen, R.Leifer, T. Novakov, J. Ogren, L.F. Radke, S.E. Schwartz, and L.. Travis, 1994: Quantifying and minimizing uncertainty of climate forcing by anthropogenic aerosols. *Bull. Am. Metorol. Soc.*, 75, 375-400.

Pinnick, R.G., G. Fernandez, E. Martinez-Andazola, B.D. Hinds, A.D.A. Hansen and K. Fuller, 1993: Aerosol in the arid southern united states: measurements of mass loading, volatility, size distribution, absorption characteristics, black carbon content, and vertical structure to 7 km above sea level. J. *Geophys. Res.*, 98, D2, 2651-2666.

Prospero, J.M., 1981: Arid regions as sources of mineral aerosols in the marine atmosphere. *Geol. Sov. of Am.*, 186, 71-86.

Prospero, J.M., and T.N. Carlson, 1972: Vertical and areal distribution of Saharan dust over the western equatorial North Atlantic Ocean. *J. Geophys. Res.*, 77, 5255-5265.

Pye, K., 1989: Processes of fine particle formation, dust source regions, and climatic changes. in: M. Leinen and M. Sarnthein (eds.), *Paleoclimatology and Paleometeorology: Modern and Past Patters of Global Atmospheric Transport*, 3-30.

Quenzel, H. and H. Müller, 1978: Optical properties of single mie particles: diagrams of intensity-extinction-scattering- and absorption efficiences. *Wiss. Mitt.* 34. Univers. Muenchen, Meteorol. Inst.

Rahn, K.A., 1981: Relative Importance of north America and Eurasia as sources of arctic aerosols. *Atmos. Environ.*, 15, 8, 1447-1455.

Rao, C.R.N., L.L. Stowe, E.P. McClain, and J. Sapper, 1988: Development and application of aerosol remote sensing with AVHRR data from NOAA satellites. In: P.V. Hobbs and M.P. McCormick (Eds.), *Aerosol and Climate*, A.Deepak Publishing, Hampton, Virginia, 69-80.

Reagan, J.A., M.V. Apte, T.V. Bruhns and O. Youngbluth, 1984: Lidar and balloon-borne cascade impactor measurements of aerosols: A case study. *Aerol. Sc. and Technol.*, 3, 259-275.

Remsberg, E.E., 1971: Radiative properties of several probable constiuents of atmospheric aerosols, *Ph. D. Thesis,* Dept. of Meteorology University of Wisconsin, Madison.

Remsberg, E.E., 1973: Stratospheric aerosol properties and their effects on infrared radiation, *J. Geophys. Res.*, 78, 1401-1407.

Roeckner, E., K. Arpe, L. Bengtsson, S. Brinkop, L. Dümenil, M. Esch, E. Kirk, F. Lunkeit, M. Ponater, B. Rockel, R. Sausen, U. Schlese, S. Schubert, M. Windelband, 1992: Simulation of the present day climate with the ECHAM-MODEL: Impact of model physics and resolution. *Max-Planck-Institut für Meteorologie, Report No.*93, Okt. 1992.

Rosen, H., T. Novakov and B.A. Bodhaine, 1981: Soot in the Artic. *Atmos. Environ.*, 15, 8, 1371-1374.

Rossknecht Rau, J.A. and M.A.K. Khalil, 1993: Anthropogenic contributions to the carbonaceous content of aerosols over the Pacific Ocean. *Atmos. Env.*, 27A, 8, 1297-1307.

Roth, W.A. and K. Scheel, Eds., 1923: Landolt-Bornstein Physikalisch-Chemische Tabellen. Springer, Berlin, 397-398.

Sasano, Y. and E.V. Browell, 1989: Light scattering characteristics of various aerosol types derived from multiple wavelength lidar observations. *Appl. Opt.*, 28, 9, 1670-1679.

Sato, M., J.E. Hansen, M.P. McCormick, and J.B. Pollack, 1993: Stratospheric Aerosol Optical Depths, 1850-1990, J. *Geophys. Res*, 98, 22,987-22,994.

Schult, I., 1992: Formation of the stratospheric aerosol layer: a global two-dimensional model. In: *Nucleation and Atmospheric Aerosols*, N. Fukuta und P.E. Wagner (Eds.), A. Deepak Publ., Hampton, S.457-460.

Schütz, L., 1979: Sahara dust transport over the North Atlantic Ocen-Model calculations and measurements. In: C. Morales (Ed.), *Saharan dust*, J. Wiley a. Sons, Chichester, 267-278.

Schütz, L., R. Jaenicke, and H. Pietrek, 1981: Saharan dust transport over the North Atlantic Ocean. *Geolog. Soc. Am. Special Paper,* 186, 87-100.

Shah, J.J., R.L. Johnson, E.K. Heyerdahl and J.J. Huntzicker, 1986: Carbonaceous aerosol at urban and rural sites in the United States, *J. Air Pollut. Control Ass*, 36, 254.

Shao, Y., M.R. Raupach, P.A. Findlater, 1993: Effect of saltation bombardment on the entrainment of dust by wind. *J. Geophys. Res.*, 98, 7, 12.719-12.726.

Shaw, G.E., 1979: Considerations on the origin and properties of the antarctic aerosol. *Rev. Geophys. Space Phys.*, 17, 8, 1983-1998.

Shaw, G.E., 1982: Atmospheric turbidity in the polar regions. *J. Appl. Meteor.*, 21, 1080-1088.

Shaw, G.E., K. Stammes and Y.X. Hu, 1993: Arctic haze: perturbation to the radiation field. *Meteorol. Atmos. Phys.*, 51, 227-235.

Shaw, Jr. R.W., and R.J. Paur, 1983: Composition of aerosol particles collected at rural sites in the Ohio River Valley. *Atmos. Environ.*, 17, 2031-2044.

Shaw, M.A. and M.J. Rood, 1990): Measurement of the crystallization humidity of ambient aerosol particles. *Atmos. Environ.*, 24A, 7, 1837-1841.
Shettle, E.P., and R.W. Fenn, 1979: Models for the aerosols of the lower atmosphere and the effect of humidity variations on their optical properties. *Air Force Geophy. Lab.*, Hanscom AFB, Mass., USA, AFGL-TR-79-0214.
Sievering, H., J. Boatman, M. Luria, and C.C. van Valin, 1989: Sulfur dry deposition over the western North Atlantic: the role of coarse aerosol particles. *Tellus,* 41B, 338-343.
Sloane, C.S., 1984: Optical properties of aerosols of mixed composition. *Atm. Environ.*, 18, 871-878.
Sloane, C.S., J. Watson, L. Pritchett, and L.W. Richards, 1991: Size-segregated fine particle measurements by chemical species and their impact on visibility impairment in Denver. *Atmos. Environ.*, 25A, 1013-1024.
Smith, M.H., P.M. Park and I.E. Consterdine, 1993: Marine aerosol concentrations and estimated fluxes over the sea. *Q.J.R. Meteorol. Soc.*, 119, 809-824.
Sokolik, I., A. Andronova and T.C. Johnson, 1993: Complex refractive index of atmsopheric dust aerosols. *Atm. Environ.*, 27A, 16, 2495-2502.
Sokolik, I.N. and G.S. Golitsyn, 1992: An investigation of the optical and radiative characteristics of dust aerosol. Izves., *Atmosp. and Ocean. Phys.*, 28, 8, 593-600.
Swap, R., M. Garstang, S. Greco, R. Talbot, P. Kallberg, 1992: Saharan dust in Amazon Basin. *Tellus,* 44B, 133-149.
Takayama, Y., and T. Takashima, 1986: Aerosol optical thickness of yellow sand over the Yellow Sea derived from NOAA satellite datsa. *Atmos. Environ.* 20, 631-638.
Talbot, R.W., M.O. Andreae and T.W. Andreae, R.C. Harriss, 1988: Regional aerosol chemistry of the Amazon Basin during the dry season. *J. Geophys. Res.*, 93, D2, 1499-1508.
Talbot, R.W., R.C. Harriss, E.V. Browell, G.L. Gregory, D.I. Sebacher, and S.M. Beck., 1986: Distribution and geochemistry of aerosols in the tropical north Atlantic troposphere: relationshio to saharan dust. *J. Geophys. Res.*, 91, D4, 5173-5182.
Tanré, D., C. Devaux, M. Herman, R. Santer and J.Y. Gac, 1988: Radiative properties of desert aerosols by optical ground-based measurements at solar wavelengths. *J. Geophys. Res.*, 93, D11, 14.223-14.231.
Tomoyuki, I., 1989: Antarctic submicron aerosols and long-range transport of pollutants. *Ambio,* 18, 1, 34-41.
Trijonis, J., 1982: Existing and natural background levels of visibility and fine particles in the rural east. *Atmos. Environ.*, 16, 10, 2431-2445.
Twitty, J. T., and J. A. Weinman, 1971: Radiative properties of carbonaceous aerosols, *J. Appl. Meteorol.*, 10, 725-731.
Volz, F.E., 1972: Infrared absorption by atmospheric aerosol substances. *J. Geophys. Res.*, 27, 1017-1031.
Volz, F.E., 1973: Infrared constants of ammonium sulfate, Sahara dust, volcanic pumice and flyash. *Appl. Opt.,* 12, 564-568.
Volz, F.E., 1983: Infrared optical constants of aerosols at some locations. *Appl. Opt.*, 22, 3690-3700.
Waggoner, A.P. and R.E. Weiss, 1980: Comparison of fine particle mass concentration and light scattering extinction in ambient aerosol. *Atmos. Environ.*, 14, 623-626.
Weast, R.C. (Ed.), 1976: *CRC Handbook of Chemistry and Physics*, CRC Press, Cleveland, Ohio.
Wendling, P., R. Wendling, W. Renger, D.S. Covert, J. Heintzenberg and P. Morel, 1985: Calculated radiative effects of arctic haze during a pollution episode in spring 1983 based on ground-based and airborne measurements. *Atmos. Environ.*, 19, 12, 2181-2193.
Whelpdale, D.M., A. Eliassen, J.N. Galloway, H. Dovland, J.M. Miller, 1988: The transatlantic transport of sulfur. *Tellus,* 40B, 1-15.
Willison, M.J., A.G. Clarke and E.M. Zeki, 1985: Seasonal variation in atmospheric aerosol concentration and composition at urban and rural sites in Northern England. *Atmos. Environ.*, 19, 1081-1089.
Winkler, P., 1973: The growth of atmospheric aerosol particles as a function of the relative humidity-II. An improved concept of mixed nuclei. *Aerosol Sci.*, 4, 373-387.
WMO, 1983: *Report of the experts meeting on aerosols and their climatic effects.* Eds. A. Deepak and H.E. Gerber. WCP-55, WMO, Geneva, 107.
Yamato, M., Y. Iwasaka, K. Okada, A. Ono, F. Nishio, and M. Fukabori, 1987: Evidence for the presence of submicron sulfuric acid particles in summer Antarctic amtosphere. *Proc. NIPR Symp. Polar Meteorol. Glaciol.*, 1, 74-81.
Yamato, M., H. Tanaka, 1994: Aircraft observations of aerosols in the free marine troposphere over the North Pacific Ocean: Particle chemistry in relation to air mass origin. *J. Geophys. Res.*, 99, D3, 5353-5377.
Zhang, J., S.M. Liu, C. Lü and W.W. Huang, 1993: Characterizing Asian wind-dust transport to the Northwest Pacific Ocean. Direct measurements of the dust flux for two years. *Tellus*, 45B, 335-345.

List of Symbols and Constants

Symbol	Definition	Unit
σ_e	Extinction coefficient	km^{-1}
σ_s	Scattering coefficient	km^{-1}
σ_a	$=\sigma_e-\sigma_s$:= Absorption coefficient	km^{-1}
ω_0	$=\frac{\sigma_s}{\sigma_e}=1-\frac{\sigma_a}{\sigma_e}$:= Single scattering albedo	
$P(\theta)$	Phase function at scattering angle θ	sr^{-1}
g	Asymmetry factor	
δ	$=\int \sigma_e dz$:= Optical depth of a column in the atmosphere	
z	Height in the atmosphere	km
ρ	Particle density	$g \cdot cm^{-3}$
λ	Wavelength	μm
N	Particle number density	cm^{-3}
M	Mass concentration	$\mu g \cdot m^{-3}$
V	Volume concentration	$cm^3 \cdot cm^{-3}$
m*	Refractive index (real and imaginary part)	
r_m	Mode radius	μm
σ	Standard deviation of the size distribution	
σ_e^*	$=\sigma_e/M$:= Mass extinction efficiency	$m^2 \cdot g^{-1}$
σ_a^*	$=\sigma_a/M$:= Mass absorption efficiency	$m^2 \cdot g^{-1}$
α	$=\ln(\sigma_{\varepsilon 1}/\sigma_{\varepsilon 2}) / \ln(\lambda_2/\lambda_1)$:= Ångström exponent	

Components of the Global Aerosol Data Set					
No.	**Aerosol Component**	**Name**	r_m [μm]	σ	ρ [g/cm^3]
1	Water-insoluble	**INSO**	4.71E-1	2.51	2.0
2	Water-soluble	**WASO**	2.12E-2	2.24	1.8
3	Soot	**SOOT**	1.18E-2	2.00	1.0
4	Sea-salt (accumulation mode)	**SSAM**	2.09E-1	2.03	2.2
5	Sea-salt (coarse mode)	**SSCM**	1.75E+0	2.03	2.2
6	Mineral (nucleus mode)	**MINM**	7.00E-2	1.95	2.6
7	Mineral (accumulation mode)	**MIAM**	3.90E-1	2.00	2.6
8	Mineral (coarse mode)	**MICM**	1.90E+0	2.15	2.6
9	Mineral-transported	**MITR**	5.00E-1	2.20	2.6
10	H_2SO_4-Droplets	**SUSO**	6.95E-2	2.03	1.7

Table 1: Aerosol components of the Global Aerosol Data Set and their main microphysical parameters.

RH [%]	0	50	70	80	90	95	98	99
WASO								
r_m [µm]	0.021	0.026	0.028	0.031	0.035	0.040	0.048	0.053
ρ [g/cm^3]	1.80	1.42	1.33	1.27	1.18	1.12	1.07	1.05
SSAM								
r_m [µm]	0.209	0.336	0.378	0.416	0.497	0.605	0.801	0.995
ρ [g/cm^3]	2.20	1.29	1.20	1.15	1.09	1.05	1.02	1.01
SSCM								
r_m [µm]	1.75	2.82	3.17	3.49	4.18	5.11	6.84	8.59
ρ [g/cm^3]	2.20	1.29	1.20	1.15	1.09	1.05	1.02	1.01
SUSO								
r_m [µm]	0.070	0.098	0.109	0.118	0.135	0.158	0.195	0.231
ρ [g/cm^3]	1.70	1.25	1.18	1.14	1.10	1.06	1.03	1.02

Table 2: Mode radius and specific density of the hygroscopic aerosol components for eight values of relative humidity RH.

	Radius Range 0.005 - 7.5 µm		Theoretical Value	
RH [%]	Volume [µm³/m³/1/m³]	Mass [µg/m³/1/cm³]	Volume [µm³/m³/1/m³]	Mass [µg/m³/1/cm³]
INSO				
	1.19E+01	2.37E+01	1.99E+01	3.98E+01
WASO				
0	7.43E-04	1.34E-03	7.43E-04	1.34E-03
50	1.40E-03	1.99E-03	1.40E-03	1.99E-03
70	1.80E-03	2.40E-03	1.80E-03	2.40E-03
80	2.23E-03	2.84E-03	2.32E-03	2.95E-03
90	3.28E-03	3.88E-03	3.28E-03	3.88E-03
95	4.95E-03	5.54E-03	4.95E-03	5.54E-03
98	8.40E-03	8.99E-03	8.41E-03	9.00E-03
99	1.19E-02	1.25E-02	1.19E-02	1.25E-02
SOOT				
	5.98E-05	5.98E-05	5.98E-05	5.98E-05
SSAM				
0	3.64E-01	8.02E-01	3.65E-01	8.03E-01
50	1.50E+00	1.93E+00	1.52E+00	1.96E+00
70	2.12E+00	2.54E+00	2.16E+00	2.59E+00
80	2.81E+00	3.23E+00	2.88E+00	3.31E+00
90	4.69E+00	5.12E+00	4.91E+00	5.35E+00
95	8.18E+00	8.59E+00	8.85E+00	9.30E+00
98	1.75E+01	1.78E+01	2.06E+01	2.10E+01
99	3.02E+01	3.05E+01	3.94E+01	3.98E+01
SSCM				
0	1.01E+02	2.23E+02	2.14E+02	4.71E+02
50	2.05E+02	2.65E+02	8.96E+02	1.16E+03
70	2..32E+02	2.78E+02	1.27E+03	1.53E+03
80	2.52E+02	2.90E+02	1.70E+03	1.96E+03
90	2.83E+02	3.09E+02	2.92E+03	3.18E+03
95	3.03E+02	3.18E+02	5.33E+03	5.60E+03
98	2.95E+02	3.01E+02	1.28E+04	1.31E+04
99	2.61E+02	2.64E+02	2.53E+04	2.56E+04
MINM				
	1.07E-02	2.78E-02	1.07E-02	2.78E-02
MIAM				
	2.13E+00	5.53E+00	2.16E+00	5.61E+00
MICM				
	1.23E+02	3.21E+02	4.01E+02	1.04E+03
MITR				
	7.37E+00	1.92E+01	8.59E+00	2.23E+01
SUSO				
0	1.34E-02	2.28E-02	1.34E-02	2.28E-02
50	3.76E-02	4.70E-02	3.76E-02	4.70E-02
70	5.18E-02	6.11E-02	5.18E-02	6.11E-02
80	6.57E-02	7.49E-02	6.57E-02	7.49E-02
90	9.83E-02	1.08E-01	9.84E-02	1.08E-01
95	1.58E-01	1.67E-01	1.58E-01	1.67E-01
98	2.96E-01	3.05E-01	2.96E-01	3.05E-01
99	4.91E-01	5.01E-01	4.938E-01	5.03E-01

Table 3: Volume and mass concentration normalised by one aerosol particle per cm^3 for all aerosol components and humidity classes for the radius range of 0.005 to 7.5 µm and for the whole radius range named by theoretical values after Equation 3.2, respectively.

Optical Parameters of Aerosol Components GADS						
Aerosol Component	λ = 0.5 μm			λ = 10 μm		
	σ_e* [m^2/g]	ω_0	g	σ_e* [m^2/g]	ω_0	g
INSO	0.21E+0	0.72	0.84	0.18E+0	0.58	0.66
WASO	0.36E+1	0.98	0.68	0.49E-1	0.04	0.16
SOOT	0.11E+2	0.23	0.35	0.35E+0	0.00	0.01
SSAM	0.13E+1	1.00	0.78	0.84E-1	0.49	0.56
SSCM	0.12E+0	1.00	0.82	0.13E+0	0.72	0.87
MINM	0.28E+1	0.95	0.67	0.91E-1	0.09	0.16
MIAM	0.55E+0	0.83	0.76	0.32E+0	0.47	0.38
MICM	0.74E-1	0.62	0.87	0.95E-1	0.52	0.69
MITR	0.26E+0	0.78	0.81	0.24E+0	0.48	0.44
SUSO	0.38E+1	1.00	0.77	0.17E+0	0.05	0.12

Table 4: Mass extinction efficiency, single scattering albedo and asymmetry factor of the aerosol components at the wavelength of 0.5 μm and 10 μm.

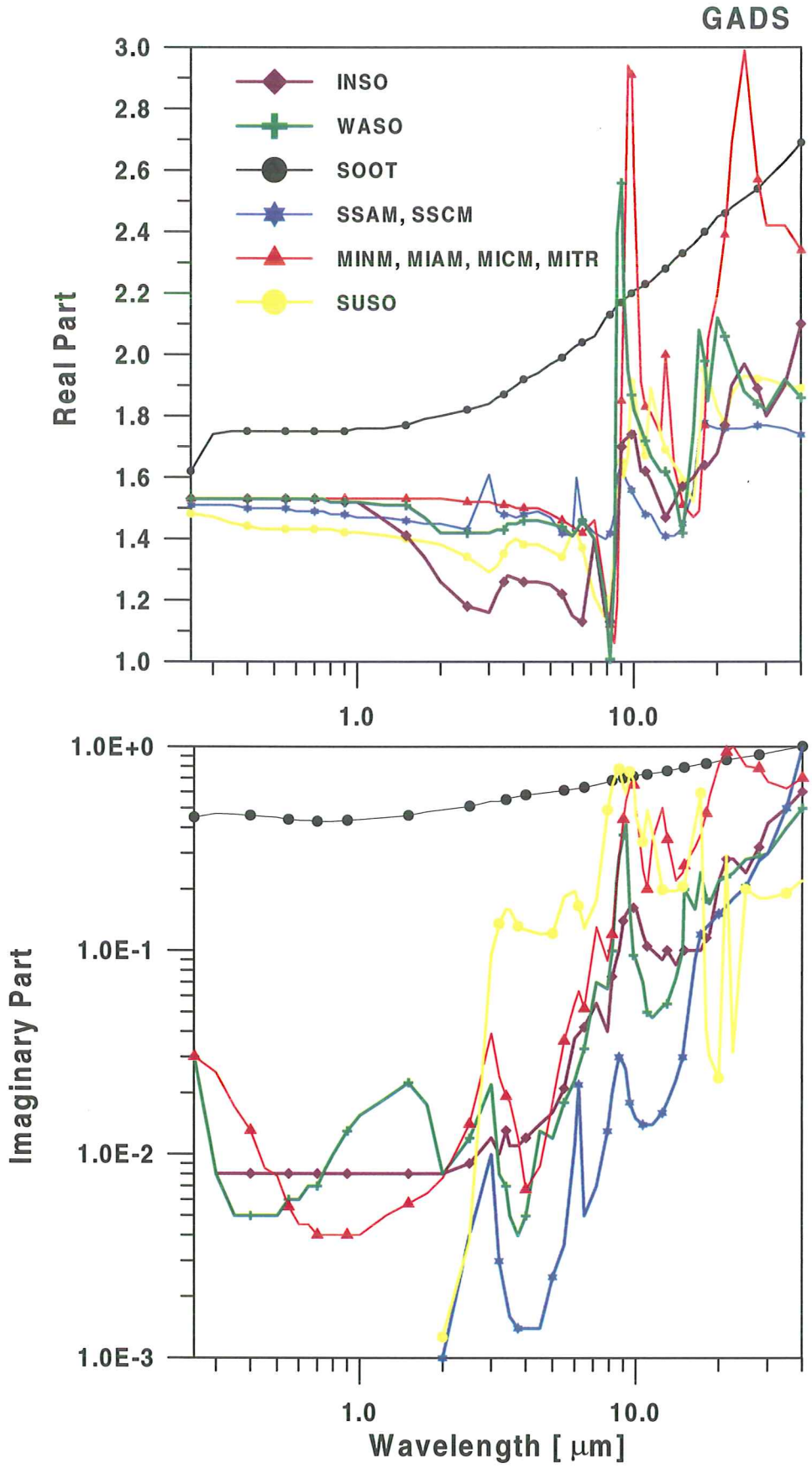

Figure 1: Complex refractive indices of aerosols dependent on the wavelength; both real part (a) and imaginary part (b).

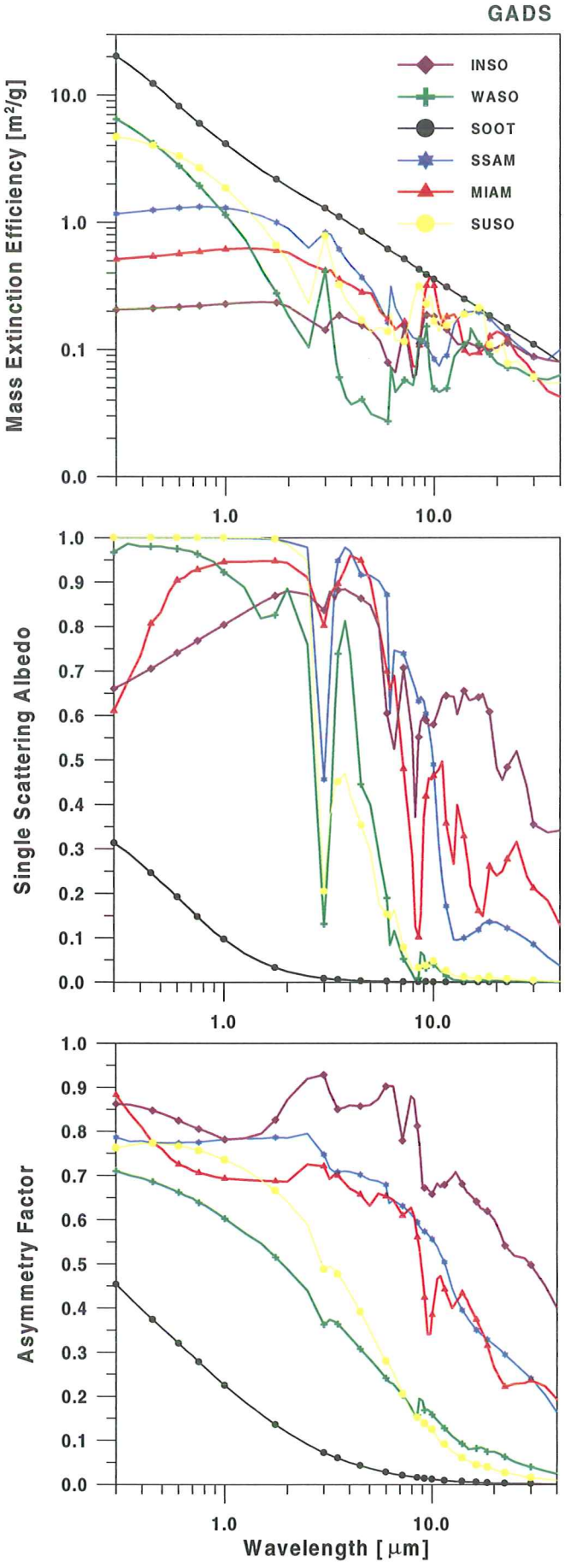

***Figure 2*:** Optical properties of the main aerosol components resulted from the Mie calculation; mass extinction efficiency [m^2/g] (a), single scattering albedo (b), and asymmetry factor (c) dependent on the wavelength.

Figure 3: Global distribution of the aerosol mass concentration [$\mu g/m^3$] of the component INSO for northern winter.

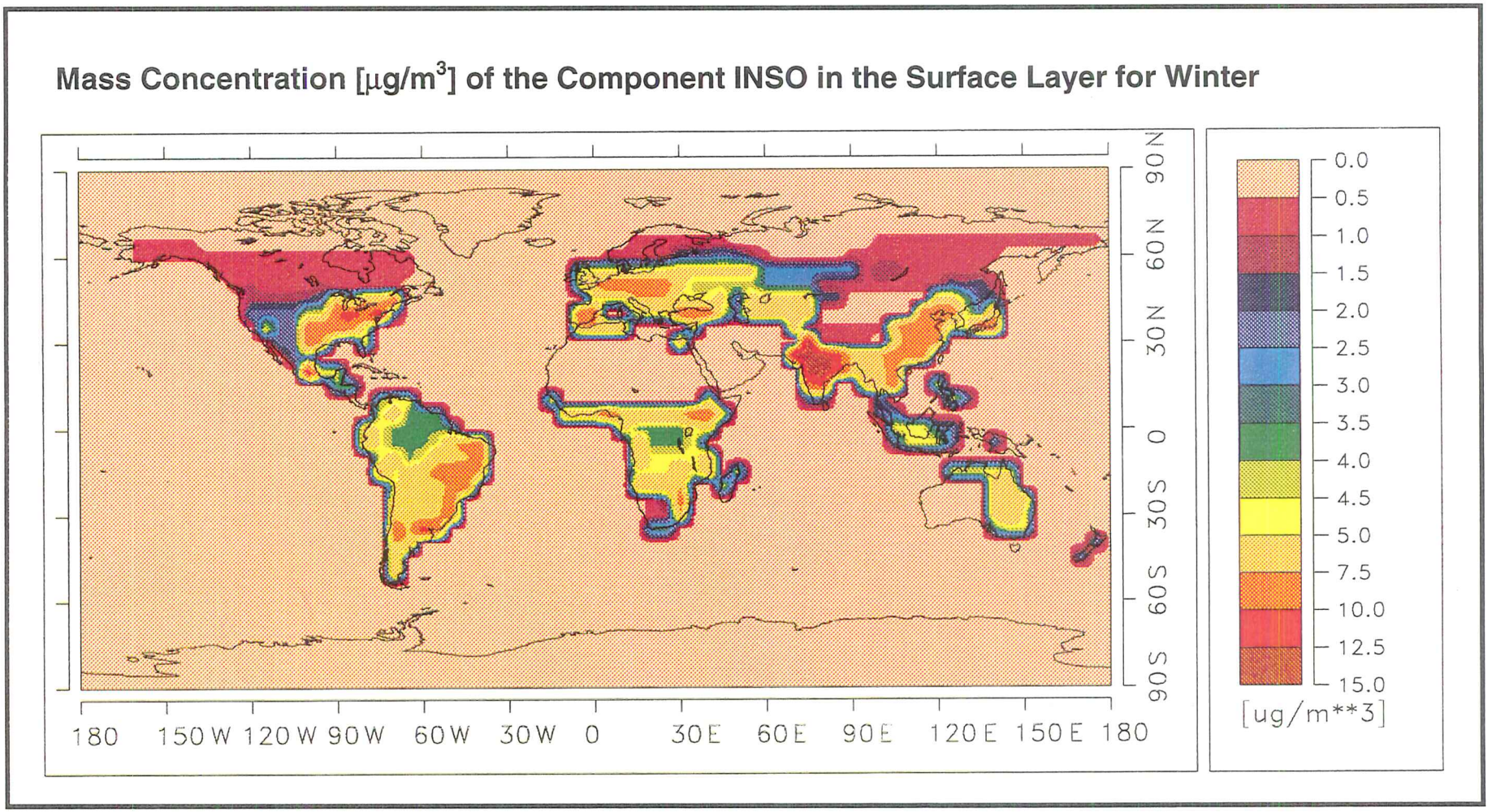

Figure 4: Global distribution of the aerosol mass concentration [μg/m^3] of the component WASO in the surface layer for winter.

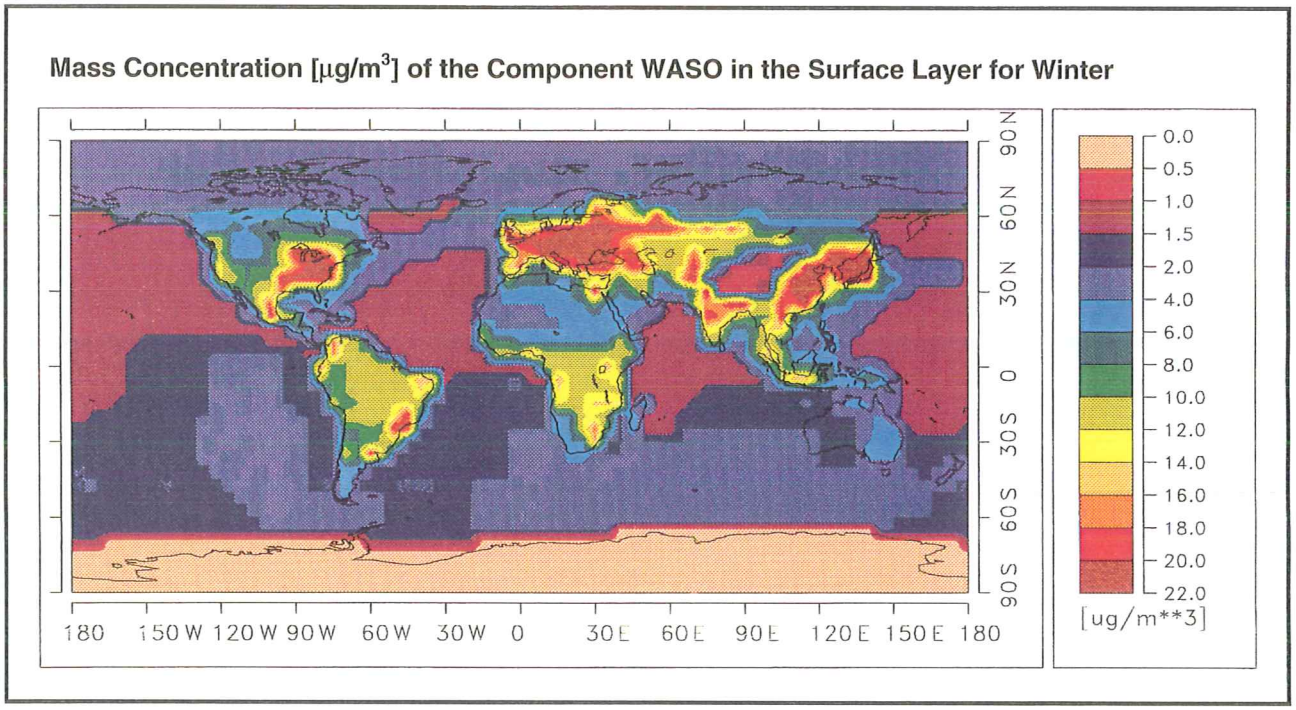

Figure 5: Global distribution of the aerosol mass concentration [μg/m^3] of the component SOOT in the surface layer for summer.

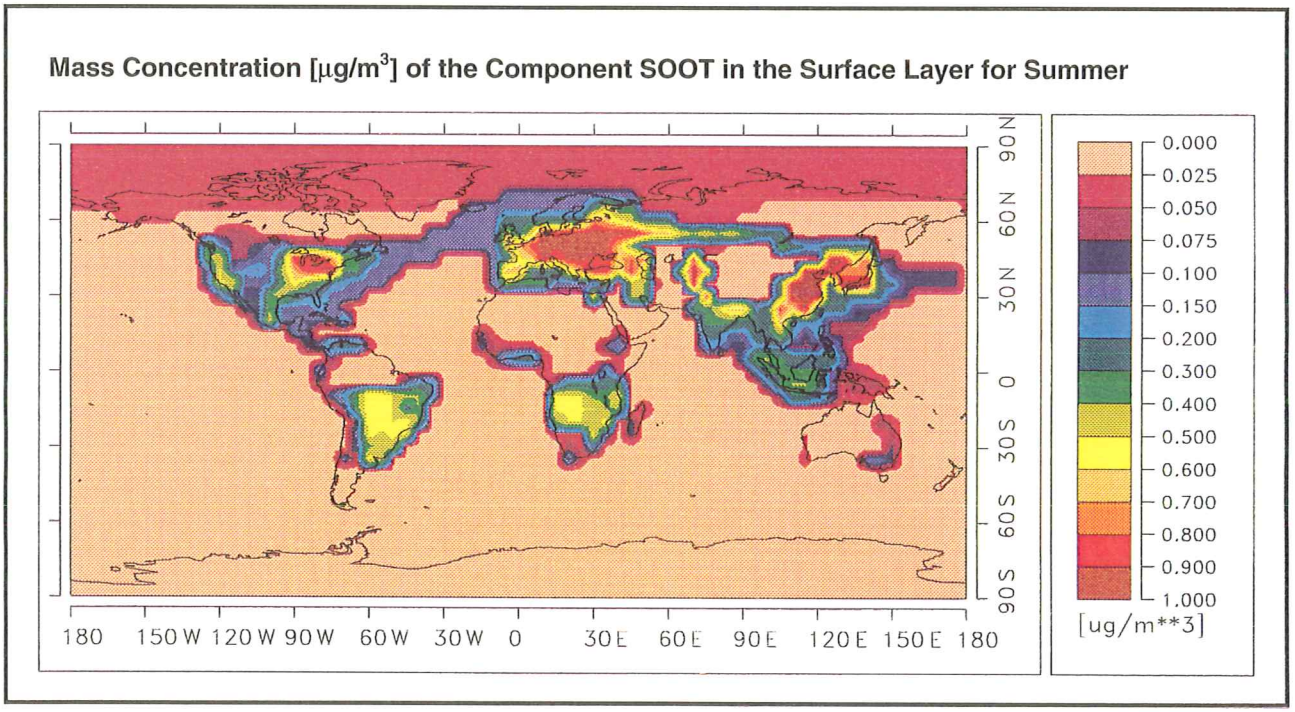

Figure 6: Global distribution of the aerosol number concentration [cm^{-3}] of the component SSAM in the surface layer for summer.

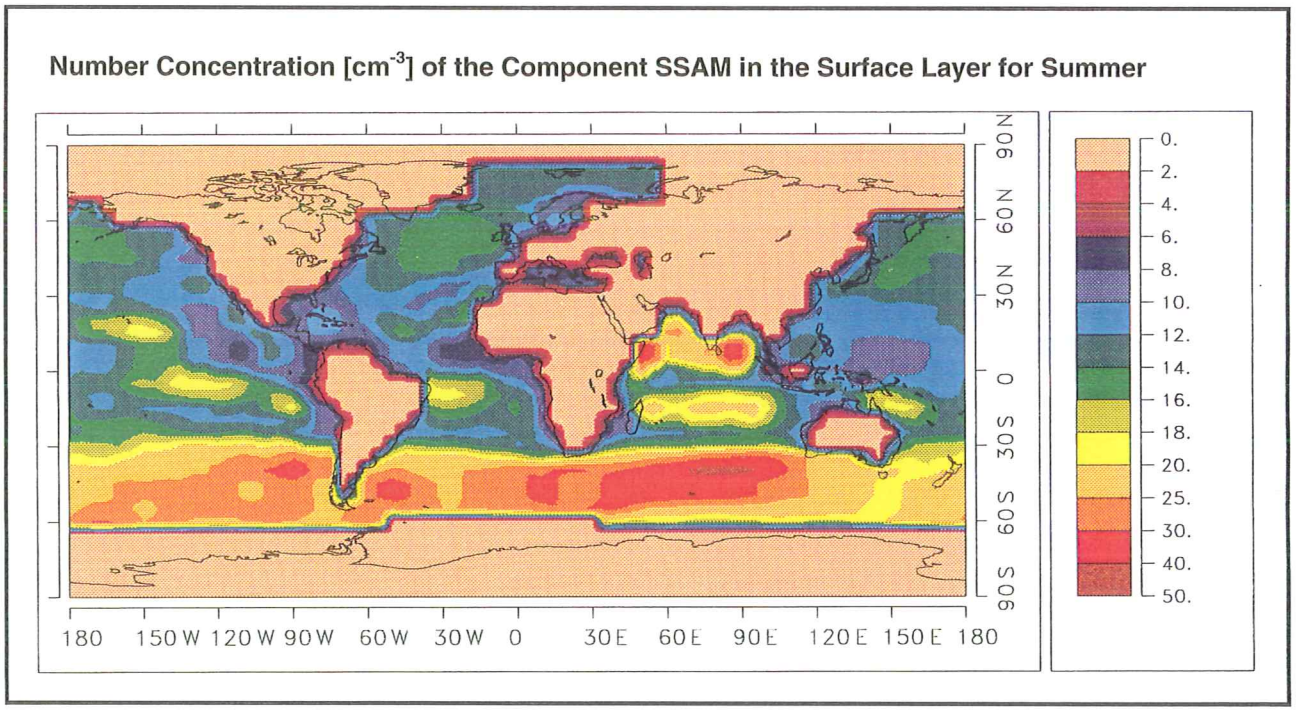

Figure 7: Global distribution of the aerosol mass concentration [cm^{-3}] of all mineral components (MINM, MIAM, MICM, MITR) in the surface layer (green to red colouring) and in the second layer of the far transport (blue colouring) for winter.

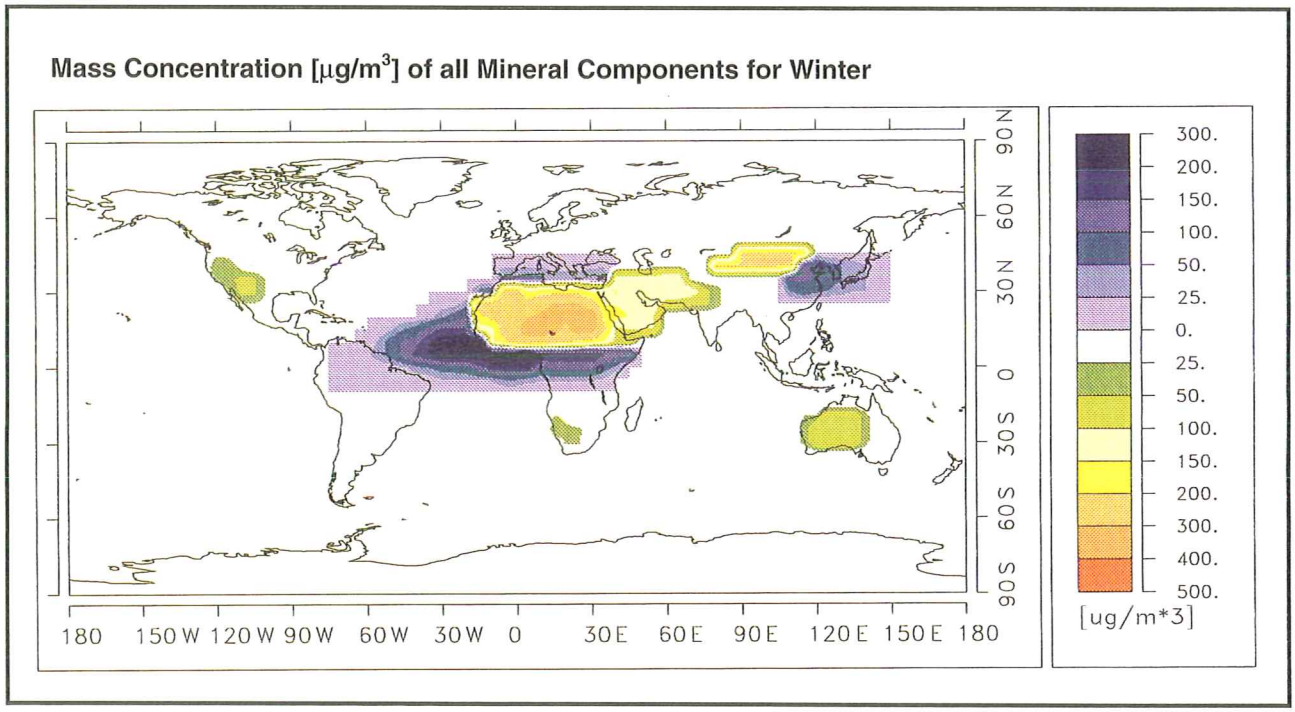

Figure 8a: Global distribution of the mass concentration [μg/m^3] of the external mixture of all aerosol components in the surface layer at the relative humidity of 50% for winter. Calculations are based on particle mass for the radius range up to 7.5 μm.

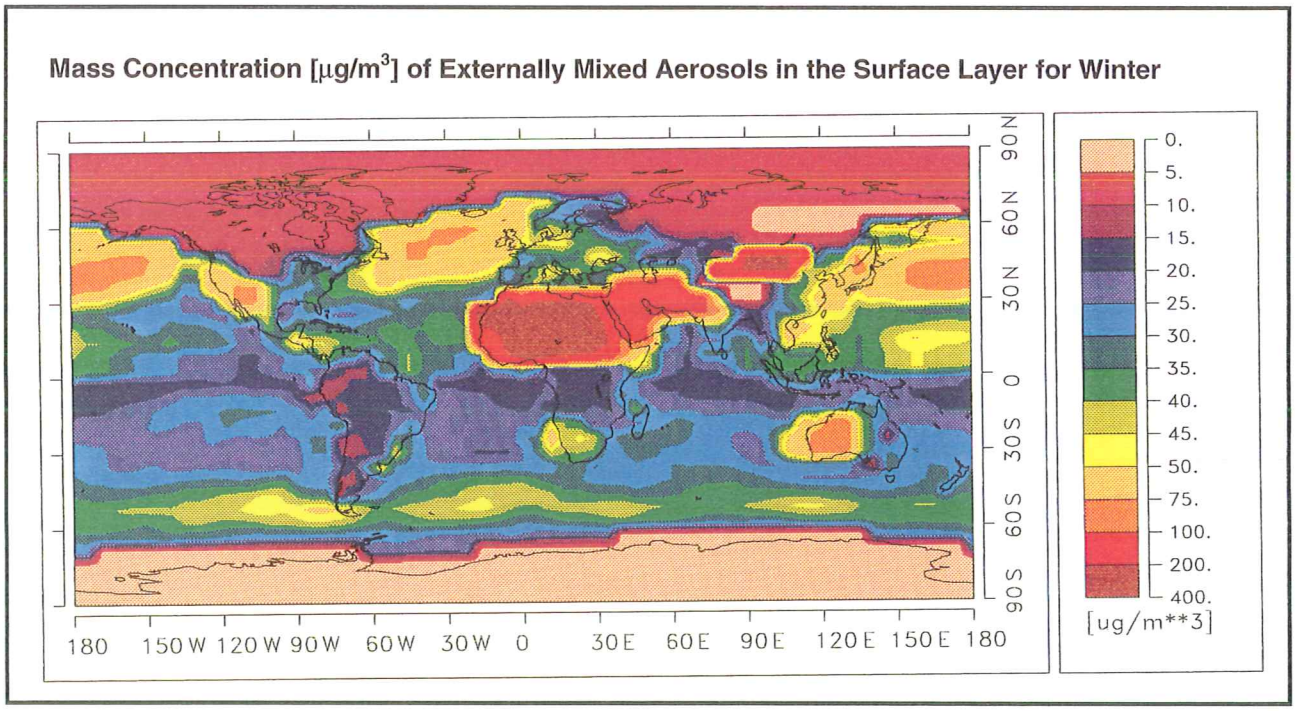

Figure 8b: Global distribution of the mass concentration [μg/m^3] of the external mixture of all aerosol components in the surface layer at the relative humidity of 50% for summer. Calculations are based on particle mass for the radius range up to 7.5 μm.

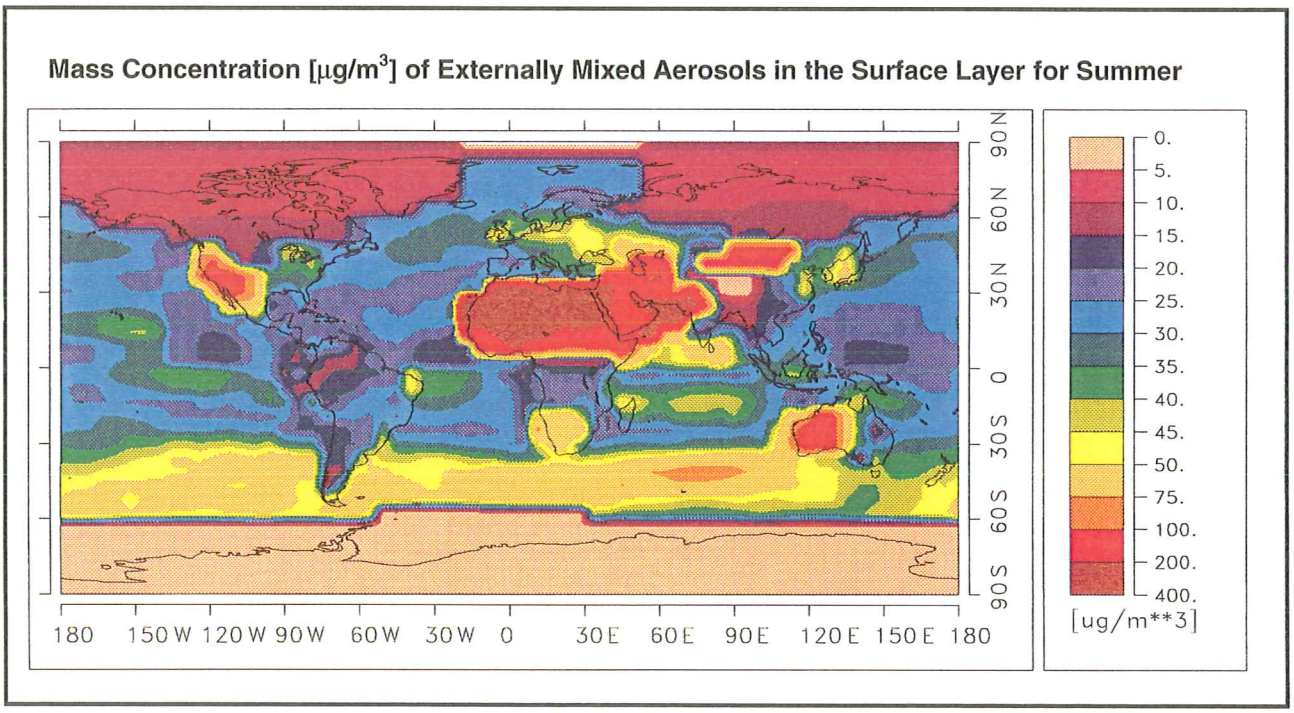

Figure 9a: Optical depth of the total aerosol at the wavelength of 0.5 µm and relative humidity of 50 % based on the Global Aerosol Data Set for winter.

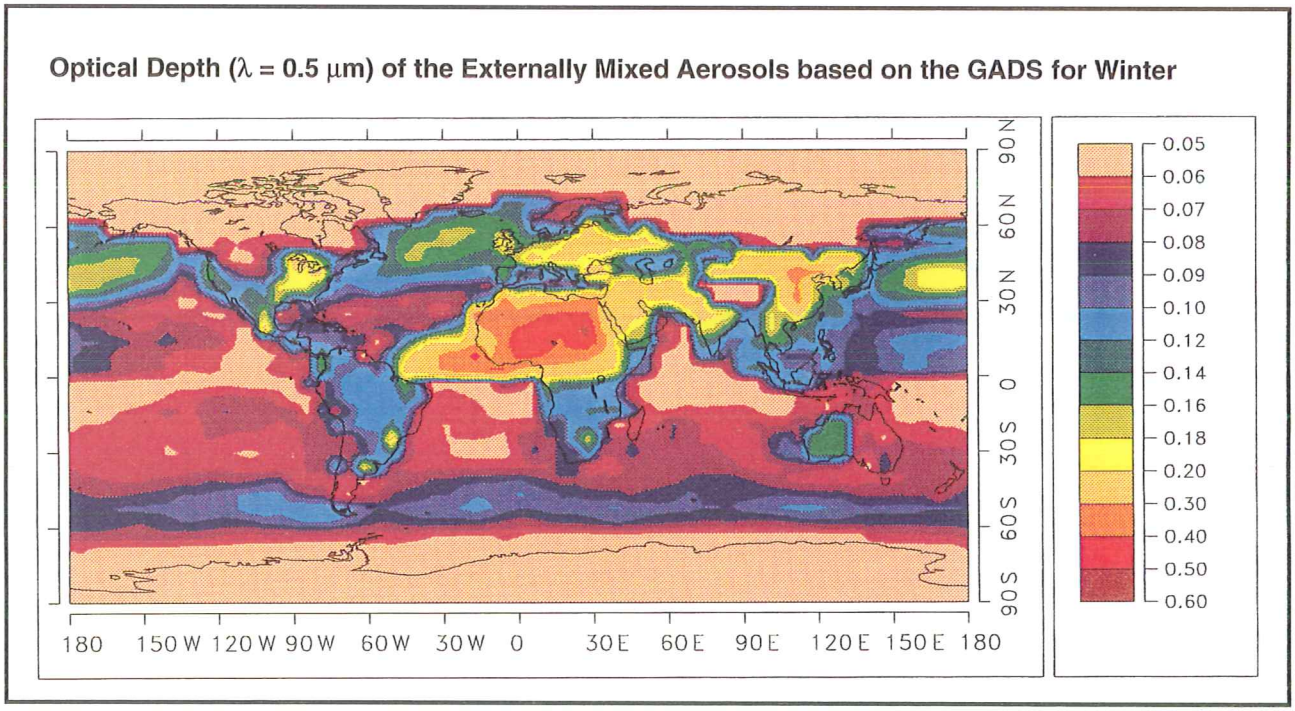

Figure 9b: Optical depth of the total aerosol at the wavelength of 0.5 µm and relative humidity of 50 % based on the Global Aerosol Data Set for summer.

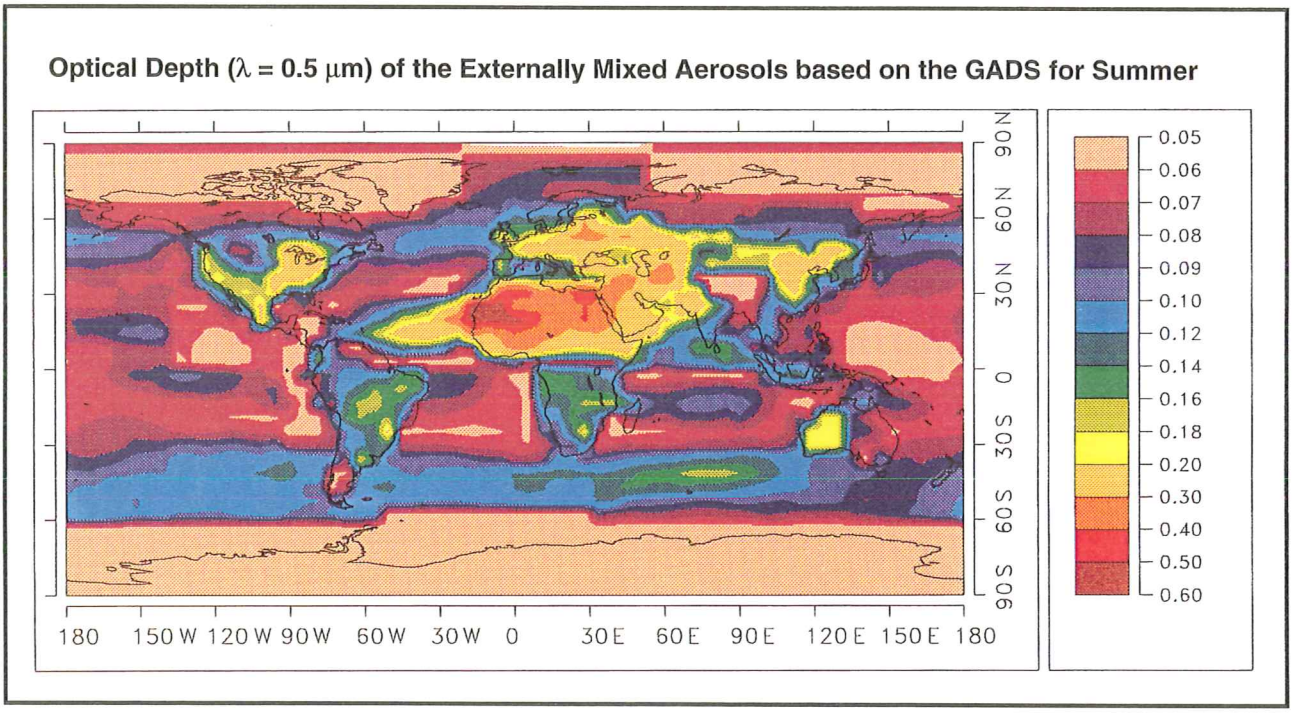

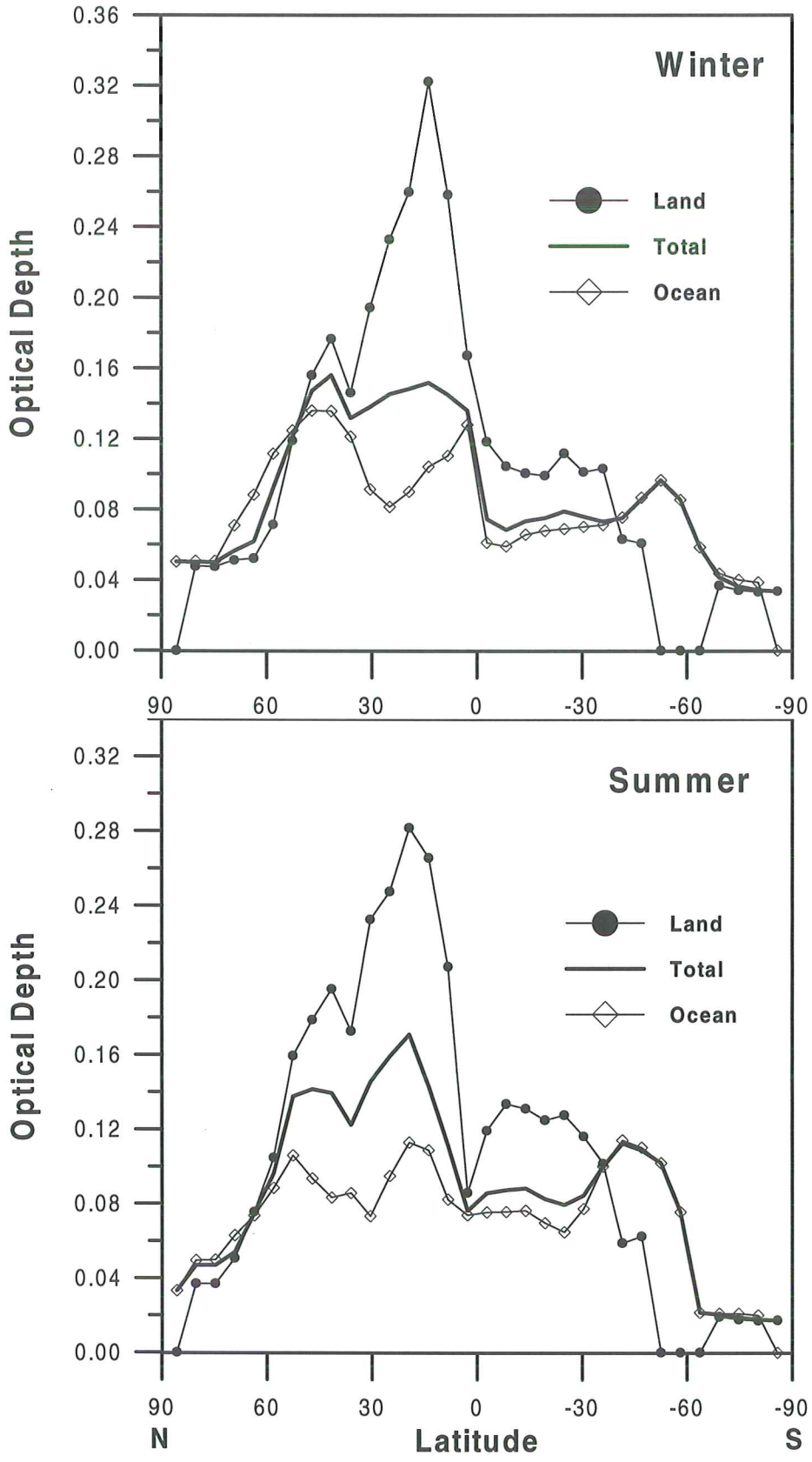

Figure 10: Zonal means of optical depth ($\lambda = 0.5$ μm) by total aerosols for winter (a) and summer (b). Zonally averaged values over land (•) and ocean (◊) are also shown.